ESAIM: M2AN 54 (2020) 391–430
https://doi.org/10.1051/m2an/2019071

ESAIM: Mathematical Modelling and Numerical Analysis
www.esaim-m2an.org

ERGODIC SDES ON SUBMANIFOLDS AND RELATED NUMERICAL SAMPLING SCHEMES

Wei Zhang*

Abstract. In many applications, it is often necessary to sample the mean value of certain quantity with respect to a probability measure μ on the level set of a smooth function $\xi : \mathbb{R}^d \to \mathbb{R}^k$, $1 \leq k < d$. A specially interesting case is the so-called conditional probability measure, which is useful in the study of free energy calculation and model reduction of diffusion processes. By Birkhoff's ergodic theorem, one approach to estimate the mean value is to compute the time average along an infinitely long trajectory of an ergodic diffusion process on the level set whose invariant measure is μ. Motivated by the previous work of Ciccotti *et al.* (*Commun. Pur. Appl. Math.* **61** (2008) 371–408), as well as the work of Leliévre *et al.* (*Math. Comput.* **81** (2012) 2071–2125), in this paper we construct a family of ergodic diffusion processes on the level set of ξ whose invariant measures coincide with the given one. For the conditional measure, we propose a consistent numerical scheme which samples the conditional measure asymptotically. The numerical scheme doesn't require computing the second derivatives of ξ and the error estimates of its long time sampling efficiency are obtained.

Mathematics Subject Classification. 65C05, 58J65.

Received May 13, 2018. Accepted September 24, 2019.

1. Introduction

Many stochastic dynamical systems in real-world applications in physics, chemistry, and biology often involve a large number of degrees of freedom which evolve on vastly different time scales. Understanding the behavior of these systems can be highly challenging due to the high dimensionality and the existence of multiple time scales. To tackle these difficulties, the terminology *reaction coordinate*, or *collective variable*, is often introduced to help describe the essential dynamical behavior of complex systems [17, 18, 26, 33, 36].

In various research topics, in particular those related to molecular dynamics, one often encounters the problem of computing the mean value of certain quantity on the level set

$$\Sigma = \xi^{-1}(\mathbf{0}) = \left\{ x \in \mathbb{R}^d \;\middle|\; \xi(x) = \mathbf{0} \in \mathbb{R}^k \right\} \tag{1.1}$$

of a reaction coordinate function $\xi : \mathbb{R}^d \to \mathbb{R}^k$, $1 \leq k < d$. Among different probability measures on Σ, the one defined by

$$\mathrm{d}\mu_1 = \frac{1}{Z} \mathrm{e}^{-\beta U} \left[\det(\nabla \xi^T \nabla \xi) \right]^{-\frac{1}{2}} \mathrm{d}\nu \tag{1.2}$$

Keywords and phrases. Ergodic diffusion process, reaction coordinate, level set, conditional probability measure.

Zuse Institute Berlin, Takustrasse 7, 14195 Berlin, Germany.
*Corresponding author: wei.zhang@fu-berlin.de

Article published by EDP Sciences

is especially relevant in applications and is sometimes called the conditional probability measure on Σ. In (1.2), the parameter $\beta > 0$, $U : \mathbb{R}^d \to \mathbb{R}$ is a smooth function, Z is the normalization constant, $\nabla\xi$ denotes the $d \times k$ Jacobian matrix of the map ξ, and ν is the surface measure on Σ induced from the Lebesgue measure on $\mathbb{R}^d$. The probability measure μ_1 has a probabilistic interpretation, and the numerical computation of the mean value

$$\overline{f} = \int_\Sigma f(x)\,\mathrm{d}\mu_1(x) \tag{1.3}$$

for a function f on the level set is involved in various contexts, such as free energy calculations based on the thermodynamics integration formula [19,30,31].

Applying Birkhoff's ergodic theorem, the mean value $\overline{f}$ can be approximated by the time average $\frac{1}{T}\int_0^T f(X_s)\,\mathrm{d}s$ along a long trajectory of the process X_s which evolves on the level set Σ and has the invariant measure μ_1. For this purpose, it is helpful to construct a diffusion process on the level set with the correct invariant measure μ_1, *i.e.*, to write down the stochastic differential equation (SDE) of X_s in $\mathbb{R}^d$. While finding such a SDE is trivial in the linear reaction coordinate case [41], it is not obvious when the reaction coordinate ξ is a nonlinear function of system's state.

In the literature, the problem finding SDEs on the level set of the reaction coordinate function with a given invariant measure has been considered in the study of free energy calculations [9,10,30,31]. Given a smooth function $U : \mathbb{R}^d \to \mathbb{R}$, the authors in [10] constructed a diffusion process Y_s on Σ whose unique invariant measure is μ_2, given by

$$\mathrm{d}\mu_2 = \frac{1}{Z}\mathrm{e}^{-\beta U}\,\mathrm{d}\nu. \tag{1.4}$$

It is also shown in [10] that this process Y_s can be obtained by projecting the dynamics

$$\mathrm{d}\widetilde{Y}_s = -\nabla U(\widetilde{Y}_s)\,\mathrm{d}s + \sqrt{2\beta^{-1}}\,\mathrm{d}W_s \tag{1.5}$$

from $\mathbb{R}^d$ onto the level set Σ, where $W_s = (W_s^1, \ldots, W_s^d)^T$ is a d-dimensional Brownian motion. The dynamics Y_s can be used to sample μ_2, and therefore to sample the conditional measure μ_1 in (1.2) as well, by either modifying the potential U or reweighting the function f according to the factor $\left[\det(\nabla\xi^T\nabla\xi)\right]^{-\frac{1}{2}}$. In a more recent work [31], the authors studied the constrained Langevin dynamics, which evolves on the submanifold of the entire phase space including both position and momentum. It is shown in [31] that the position components of the constrained Langevin dynamics has the marginal invariant measure which coincides with μ_2. Therefore, it can also be used to compute the average $\overline{f}$ with respect to the conditional measure μ_1 (by either modifying the potential or reweighting f according to $\left[\det(\nabla\xi^T\nabla\xi)\right]^{-\frac{1}{2}}$). Detailed studies on the numerical schemes as well as applications of the constrained Langevin dynamics have been carried out in [31].

The same conditional probability measure μ_1 in (1.2), as well as the average $\overline{f}$ in (1.3), also plays an important role in the study of the effective dynamics of diffusion processes [14,24,26,44]. As a generalization of the dynamics (1.5), the diffusion process

$$\mathrm{d}\widetilde{Y}_s^i = -\left(a_{ij}\frac{\partial U}{\partial x_j}\right)(\widetilde{Y}_s)\,\mathrm{d}s + \frac{1}{\beta}\frac{\partial a_{ij}}{\partial x_j}(\widetilde{Y}_s)\,\mathrm{d}s + \sqrt{2\beta^{-1}}\sigma_{ij}(\widetilde{Y}_s)\,\mathrm{d}W_s^j, \quad 1 \le i \le d, \tag{1.6}$$

and its effective dynamics have been considered in [44], where the matrix-valued coefficients $\sigma, a : \mathbb{R}^d \to \mathbb{R}^{d\times d}$ are related by $a = \sigma\sigma^T$, such that a is uniformly positive definite. Notice that, (1.6) is written in component-wise form with Einstein's summation convention (the same Einstein's summation convention will be used throughout this paper, whenever no ambiguity will arise), and it reduces to (1.5) when $\sigma = a = \mathrm{id}$. The infinitesimal generator of (1.6) can be written as

$$\mathcal{L} = \frac{\mathrm{e}^{\beta U}}{\beta}\frac{\partial}{\partial x_i}\left(\mathrm{e}^{-\beta U}a_{ij}\frac{\partial}{\partial x_j}\right). \tag{1.7}$$

Under mild conditions on U, it is known that, for any (smooth, uniformly positive definite) coefficient a, the dynamics (1.6) has the common unique invariant measure whose probability density is $\frac{1}{Z}\mathrm{e}^{-\beta U}$ with respect to the Lebesgue measure on $\mathbb{R}^d$.

Motivated by these previous work, in this paper we try to answer the following two questions.

(Q1) *Besides the process constructed in [10] that is closely related to (1.5), can we obtain other diffusion processes on Σ, which are probably related to (1.6) involving the coefficients σ, a, and have the same invariant measure? In particular, can we construct SDEs on Σ whose invariant measure is μ_1?*

(Q2) *Numerically, instead of sampling μ_2, can we directly estimate the mean value in (1.3) with respect to μ_1, preferably with a numerical algorithm that is easy to implement?*

The main contributions of the current work are related to the above questions and are summarized below. First, concerning Question (Q1), in Theorem 2.3 of Section 2, we will construct a family of diffusion processes on Σ which sample either μ_1 or μ_2. In particular, we show that the diffusion process

$$\mathrm{d}X_s^i = -(Pa)_{ij}\frac{\partial U}{\partial x_j}\,\mathrm{d}s + \frac{1}{\beta}\frac{\partial (Pa)_{ij}}{\partial x_j}\,\mathrm{d}s + \sqrt{2\beta^{-1}}\,P_{j,i}\,\mathrm{d}W_s^j, \quad 1 \le i \le d, \tag{1.8}$$

evolves on Σ and the invariant measure is the conditional probability measure μ_1 in (1.2), where the projection map P and the invertible $k \times k$ symmetric matrix Ψ are given by

$$P = \mathrm{id} - a\nabla\xi\Psi^{-1}\nabla\xi^T, \quad \Psi = \nabla\xi^T a \nabla\xi. \tag{1.9}$$

Correspondingly, the infinitesimal generator of (1.8) is

$$\mathcal{L} = \frac{\mathrm{e}^{\beta U}}{\beta}\frac{\partial}{\partial x_i}\left(\mathrm{e}^{-\beta U}(Pa)_{ij}\frac{\partial}{\partial x_j}\right), \tag{1.10}$$

which should be compared to the infinitesimal generator in (1.7). Second, concerning Question (Q2), in Section 3 we study a numerical algorithm which estimates the mean value $\overline{f}$ in (1.3). Specifically, we propose to use the numerical scheme

$$\begin{aligned} x_i^{(l+\frac{1}{2})} &= x_i^{(l)} + \left(-a_{ij}\frac{\partial U}{\partial x_j} + \frac{1}{\beta}\frac{\partial a_{ij}}{\partial x_j}\right)(x^{(l)})\,h + \sqrt{2\beta^{-1}h}\,\sigma_{ij}(x^{(l)})\,\eta_j^{(l)}, \quad 1 \le i \le d, \\ x^{(l+1)} &= \Theta\big(x^{(l+\frac{1}{2})}\big), \end{aligned} \tag{1.11}$$

with $x^{(0)} \in \Sigma$, and to approximate $\overline{f}$ by $\widehat{f}_n = \frac{1}{n}\sum_{l=0}^{n-1} f(x^{(l)})$. In (1.11), h is the step-size, $\boldsymbol{\eta}^{(l)} = (\eta_1^{(l)}, \eta_2^{(l)}, \ldots, \eta_d^{(l)})^T$ are independent d-dimensional standard Gaussian random variables, and $\Theta(x) = \lim_{s\to+\infty}\varphi(x,s)$ is the limit of the flow map

$$\frac{\mathrm{d}\varphi(x,s)}{\mathrm{d}s} = -(a\nabla F)\big(\varphi(x,s)\big), \quad \varphi(x,0) = x, \qquad \forall\, x \in \mathbb{R}^d, \tag{1.12}$$

with $F(x) = \frac{1}{2}|\xi(x)|^2 = \frac{1}{2}\sum_{\alpha=1}^k \xi_\alpha^2(x)$. Following the approach developed in [35], in Theorem 3.5, we obtain the estimates of the approximation error between $\widehat{f}_n$ and $\overline{f}$. While different constraint approaches have been proposed in the literature [27, 31, 43], to the best of the author's knowledge, constraint using the flow map φ has not been studied yet.

Let us comment on the two contributions mentioned above. First, knowing the SDE (1.8) and the expression (1.10) of its infinitesimal generator $\mathcal{L}$ is helpful for analysis. In fact, in Section 3, the analysis of sampling error estimate of the scheme (1.11) relies on Poisson equation on Σ related to $\mathcal{L}$ in (1.10). Furthermore, (1.10) plays a role in the work [29] in analyzing the approximation quality of the effective dynamics, while SDE (1.8) has been used in [19] to study fluctuation relations and Jarzynski's equality for nonequilibrium systems. Second,

we emphasize that $\Theta(x)$ in the scheme (1.11) can be evaluated by solving the ODE (1.12) starting from x. Although Θ is defined as the limit when $s \to +\infty$, in many cases the computational cost is not large, due to the exponential convergence of the (gradient) flow (1.12) to its limit, particularly for the initial state $x = x^{(l+\frac{1}{2})}$ that is close to Σ. Furthermore, comparing to the direct (Euler–Maruyama) discretization of SDE (1.8) which may deviate from Σ and requires second order derivatives of ξ, the scheme (1.11) satisfies $x^{(l)} \in \Sigma$ for all $l \geq 0$, and it doesn't require computing the second order derivatives of ξ. Therefore, we expect the numerical scheme (1.11) and (1.12) is both stable and relatively easy to implement. Readers are referred to Remarks 3.2 and 3.3 in Section 3 and Example 1 in Section 4 for further algorithmic discussions.

In the following, we briefly explain the approach that we will use to study Question (Q1), as well as the idea behind the scheme (1.11) and (1.12). Concerning Question (Q1), we take the manifold point of view by considering $\mathbb{R}^d$ as a Riemannian manifold $\mathcal{M} = (\mathbb{R}^d, g)$ with the metric $g = a^{-1}$, defined by

$$g(\boldsymbol{u}, \boldsymbol{v}) = \langle \boldsymbol{u}, \boldsymbol{v} \rangle_g = u_i (a^{-1})_{ij} v_j, \quad \forall\, \boldsymbol{u}, \boldsymbol{v} \in \mathbb{R}^d. \tag{1.13}$$

A useful observation is that, for $\mathcal{L}$ in (1.7), we have [44]

$$\mathcal{L} f = \left[-\mathrm{grad}^{\mathcal{M}} \left(U + \frac{1}{2\beta} \ln G \right) + \frac{1}{\beta} \Delta^{\mathcal{M}} \right] f, \quad \forall \text{ smooth } f : \mathbb{R}^d \to \mathbb{R},$$

where $G = \det g$, and $\mathrm{grad}^{\mathcal{M}}$, $\Delta^{\mathcal{M}}$ denote the gradient and the Laplacian–Beltrami operator on $\mathcal{M}$, respectively. Accordingly, (1.6) can be written as a SDE on $\mathcal{M}$ as

$$\mathrm{d}\widetilde{Y}_s = -\mathrm{grad}^{\mathcal{M}} \left(U + \frac{1}{2\beta} \ln G \right) \mathrm{d}s + \sqrt{2\beta^{-1}} \mathrm{d}\widetilde{B}_s, \tag{1.14}$$

where $\widetilde{B}_s$ is the Brownian motion on $\mathcal{M}$ [20]. Conversely, SDE (1.6) can be seen as the equation of (1.14) under the (global) coordinate chart of $\mathcal{M}$. This equivalence allows us to study (1.6) on $\mathbb{R}^d$ by the corresponding SDE (1.14) on manifold $\mathcal{M}$. Comparing to (1.6), one advantage of working with the abstract equation (1.14) is that the invariant measure of (1.14) can be recognized as easily as in (1.5), provided that we apply integration by parts formula on the manifold $\mathcal{M}$.

A family of ergodic SDEs on Σ (*i.e.*, Question (Q1)) is obtained by taking the same manifold point of view. Specifically, consider Σ as a submanifold of $\mathcal{M}$ and denote by grad^{Σ}, Δ^{Σ}, B_s the gradient operator, the Laplacian and the Brownian motion (with generator $\frac{1}{2}\Delta^{\Sigma}$ [20]) on Σ, respectively. Since the infinitesimal generator of the SDE

$$\mathrm{d}Y_s = -\mathrm{grad}^{\Sigma} U \, \mathrm{d}s + \sqrt{2\beta^{-1}} \mathrm{d}B_s \tag{1.15}$$

is $\mathcal{L} = -\mathrm{grad}^{\Sigma} U + \frac{1}{\beta} \Delta^{\Sigma}$, under mild assumptions on U, it is straightforward to verify that dynamics (1.15) evolves on Σ and has the unique invariant measure $\frac{1}{Z} \mathrm{e}^{-\beta U} \, \mathrm{d}\nu_g$, where ν_g is the surface measure on Σ induced from the metric $g = a^{-1}$ on $\mathcal{M} = (\mathbb{R}^d, g)$. Therefore, answering Question (Q1) boils down to calculating the expression of (1.15) under the coordinate chart of $\mathcal{M}$ (not Σ). This will be achieved by calculating the expressions of grad^{Σ}, Δ^{Σ} under the coordinate chart of $\mathcal{M}$ and then figuring out the relation between the two measures ν and ν_g.

Concerning the idea behind the numerical scheme (1.11) and (1.12), we recall that one way to (approximately) sample μ_1 on Σ is to constrain the dynamics (1.6) in the neighborhood of Σ by adding an extra potential to it. This is often termed as softly constrained dynamics [10, 34] and has been widely used in applications. In this context, one consider the dynamics

$$\mathrm{d}X_s^{\epsilon,i} = \left[-a_{ij} \frac{\partial U}{\partial x_j} - \frac{1}{\epsilon} a_{ij} \frac{\partial}{\partial x_j} \left(\frac{1}{2} \sum_{\alpha=1}^{k} \xi_\alpha^2 \right) + \frac{1}{\beta} \frac{\partial a_{ij}}{\partial x_j} \right] \mathrm{d}s + \sqrt{2\beta^{-1}} \sigma_{ij} \, \mathrm{d}W_s^j, \tag{1.16}$$

where $\epsilon > 0$, $1 \leq i \leq d$, based on the fact that the invariant measure of (1.16) converges weakly to μ_1, as $\epsilon \to 0$. The dynamics (1.16) stays close to Σ most of the time, thanks to the existence of the extra constraint force.

Furthermore, only the first order derivatives of ξ are involved. In spite of these nice properties, however, direct simulation of (1.16) is inefficient when ϵ is small, because the time step-size in numerical simulations becomes severely limited due to the strong stiffness in the dynamics. Indeed, our numerical scheme is motivated in order to overcome the aforementioned drawback of the softly constrained dynamics (1.16), and the scheme (1.11) and (1.12) can be viewed as a multiscale numerical method for (1.16), where the stiff and non-stiff terms in (1.16) are handled separately [41]. In contrast to the previous work [10, 13, 22], where the convergence of (1.16) was studied on a finite time interval, our result concerns the long time sampling efficiency of the discretized numerical scheme.

Before concluding this introduction, we compare the current work with several previous ones. Generally speaking, Monte Carlo samplers (based on ergodicity) either on $\mathbb{R}^d$ or on its submanifolds can be classified into Metropolis-adjusted samplers and samplers without Metropolis step (unadjusted). For Metropolis-adjusted methods, in particular, exploiting Riemannian geometry structure to develop MCMC methods has been studied in [16]. The authors there demonstrated that incorporating the geometry of the space into numerical methods can lead to significant improvement of the sampling efficiency. In line with this development, in Section 4 we will consider a concrete example where a non-constant matrix a can help remove the stiffness in the sampling task. On the other hand, despite of the common Riemannian manifold point of view in the current work and in [16], the main difference is that the current work deals with sampling on the submanifold Σ instead of the entire $\mathbb{R}^d$ (or its domain). The derivations in the current work are more involved mainly due to this difference. Besides sampling on the entire space, Metropolis-adjusted samplers on submanifolds, using either MCMC or Hybrid Monte Carlo, have been considered in several recent work [8, 31, 32, 43]. Reversible Metropolis random walk on submanifolds has been constructed in [43], which is then extended in [32] by allowing non-zero gradient forces in the proposal move. In contrast to these Metropolis-adjusted samplers, the numerical scheme (1.11) and (1.12) in the current work is unadjusted (without Metropolis-step) and samples the conditional probability measure μ_1 when the step-size $h \to 0$. This means that in practice the step-size h should be chosen properly such that the discretization error is tolerable. In this direction, we point out that unadjusted samplers on $\mathbb{R}^d$, which naturally arise from discretizations of SDEs, have been well studied in the literature [1, 7, 11, 28, 35, 40]. The current work can be thought as a further step along this direction for sampling schemes on submanifolds, by applying the machinery developed in [35]. Comparison between the scheme (1.11) and the Metropolis-adjusted algorithm in [43] can be found in Remark 3.9, as well as in Example 2 in Section 4. We also refer to [28] for related discussions.

The rest of the paper is organized as follows. In Section 2, we construct ergodic SDEs on Σ which sample either μ_1 or μ_2. In Section 3, we study the numerical scheme (1.11) and (1.12) and quantify its approximation error in estimating the mean value in (1.3). In Section 4, we demonstrate our results through concrete examples. Conclusions and further discussions are made in Section 5. Technical details related to the Riemannian manifold $\mathcal{M}$ in Section 2 are included in Appendix A. Proofs of the results in Section 3 are collected in Appendix B.

Finally, we conclude this introduction with the assumptions which will be made (implicitly) throughout this paper.

Assumption 1.1. *The matrix $\sigma : \mathbb{R}^d \to \mathbb{R}^{d\times d}$ is both smooth and invertible at each $x \in \mathbb{R}^d$. The matrix $a = \sigma\sigma^T$ is uniformly positive definite with uniformly bounded inverse a^{-1}.*

Assumption 1.2. *The function $\xi : \mathbb{R}^d \to \mathbb{R}^k$ is C^2 smooth and the level set Σ is both connected and compact, such that rank$(\nabla\xi) = k$ at each $x \in \Sigma$.*

2. SDEs of ergodic diffusion processes on Σ

In this section, we construct SDEs of ergodic processes on Σ that sample a given invariant measure. The main result of this section is Theorem 2.3, which shows that the invariant measure of the SDE (1.8) in Introduction is the conditional probability measure μ_1 in (1.2). Readers who are mainly interested in numerical algorithms can read Theorem 2.3 and then directly jump to Section 3.

First of all, let us point out that, the semigroup approach based on functional inequalities on Riemannian manifolds is well developed to study the solution of Fokker-Planck equation towards equilibrium. One sufficient condition for the exponential convergence of the Fokker-Planck equation (and therefore the ergodicity of the corresponding dynamics) is the famous Bakry-Emery criterion [4]. In particular, concrete conditions are given in [39] which guarantee the exponential convergence to the unique invariant measure. In the following, we will always assume that the potential $U \in C^\infty(\Sigma)$ and the Bakry-Emery condition in [39] is satisfied.

Recall that $\mathcal{M} = (\mathbb{R}^d, g)$, where $g = a^{-1}$ and ν_g is the surface measure on Σ induced from $\mathcal{M}$. Matrices P, $P_{j,i}$ are given in (A.7) and (A.10), respectively. For $1 \le i \le d$, $\boldsymbol{e}_i$ denotes the vector whose ith component equals to 1 while all the other $d-1$ components equal to 0. We refer the reader to Appendix A for further details. Let us first consider the probability measure μ on Σ given by $\mathrm{d}\mu = \frac{1}{Z}\mathrm{e}^{-\beta U}\,\mathrm{d}\nu_g$, where $\beta > 0$ and Z is a normalization constant. The following proposition is a direct application of Proposition A.3.

Proposition 2.1. *Consider the dynamics on $\mathbb{R}^d$ which satisfies the Ito SDE*

$$\mathrm{d}Y_s^i = -(Pa)_{ij}\frac{\partial\left[U - \frac{1}{2\beta}\ln\left((\det a)^{-1}\det(\nabla\xi^T a\nabla\xi)\right)\right]}{\partial x_j}\,\mathrm{d}s + \frac{1}{\beta}\frac{\partial(Pa)_{ij}}{\partial x_j}\,\mathrm{d}s + \sqrt{2\beta^{-1}}\,P_{j,i}\,\mathrm{d}W_s^j \tag{2.1}$$

for $1 \le i \le d$, where $W_s = (W_s^1, W_s^2, \dots, W_s^d)^T$ is a d-dimensional Brownian motion. Suppose $Y_0 \in \Sigma$, then $Y_s \in \Sigma$ almost surely for $s \ge 0$. Furthermore, it has a unique invariant measure μ given by $\mathrm{d}\mu = \frac{1}{Z}\mathrm{e}^{-\beta U}\,\mathrm{d}\nu_g$.

Proof. Using (A.10) and Proposition A.3, we know that the infinitesimal generator of SDE (2.1) is

$$\mathcal{L}f = -\langle \mathrm{grad}^\Sigma U, \mathrm{grad}^\Sigma f\rangle_g + \frac{1}{\beta}\Delta^\Sigma f, \quad \forall\ f : \Sigma \to \mathbb{R}, \tag{2.2}$$

where grad^Σ, Δ^Σ are the gradient and Laplace–Beltrami operators on Σ of $\mathcal{M}$, respectively. Applying Ito's formula to $\xi_\alpha(Y_s)$, we have

$$\mathrm{d}\xi_\alpha(Y_s) = \mathcal{L}\xi_\alpha(Y_s)\,\mathrm{d}s + \sqrt{2\beta^{-1}}\frac{\partial\xi_\alpha(Y_s)}{\partial x_i}P_{j,i}\mathrm{d}W_s^j, \quad 1 \le \alpha \le k.$$

Using (2.2), (A.10), and the fact that $\mathrm{grad}^\Sigma\xi_\alpha = P\mathrm{grad}^{\mathcal{M}}\xi_\alpha = 0$, it is straightforward to verify that

$$\begin{aligned}\mathcal{L}\xi_\alpha &= -\langle \mathrm{grad}^\Sigma U, \mathrm{grad}^\Sigma\xi_\alpha\rangle_g + \frac{1}{\beta}\mathrm{div}^\Sigma(\mathrm{grad}^\Sigma\xi_\alpha) = 0,\\ \frac{\partial\xi_\alpha}{\partial x_i}P_{j,i} &= 0, \quad 1 \le j \le d,\end{aligned}$$

on Σ, which implies $\mathrm{d}\xi_\alpha(Y_s) = 0$, $\forall s \ge 0$. Since $Y_0 \in \Sigma$, we conclude that $\xi_\alpha(Y_s) = \xi_\alpha(Y_0) = 0$ *a.s.* $s \ge 0$, for $1 \le \alpha \le k$, and therefore $Y_s \in \Sigma$ for $s \ge 0$, almost surely.

Using the expression (2.2) of $\mathcal{L}$ and the integration by parts formula (A.15), it is easy to see that μ is an invariant measure of the dynamics (2.1). The uniqueness is implied by the exponential convergence result established in Remark 1.1 and Corollary 1.5 of [39], since we assume Bakry-Emery condition is satisfied. □

In the above, we have considered the level set Σ as a submanifold of $\mathcal{M} = (\mathbb{R}^d, g)$. In applications, on the other hand, it is natural to view Σ as a submanifold of the standard Euclidean space $\mathbb{R}^d$, with the surface measure ν on Σ that is induced from the Euclidean metric on $\mathbb{R}^d$. As already mentioned in the Introduction, the following two probability measures

$$\mathrm{d}\mu_1 = \frac{1}{Z}\mathrm{e}^{-\beta U}\left[\det(\nabla\xi^T\nabla\xi)\right]^{-\frac{1}{2}}\,\mathrm{d}\nu, \qquad \mathrm{d}\mu_2 = \frac{1}{Z}\mathrm{e}^{-\beta U}\,\mathrm{d}\nu, \tag{2.3}$$

where Z denotes possibly different normalization constants, are often interesting and arise in many situations [9, 10, 26, 44]. In particular, μ_1 has a probabilistic interpretation and often appears in the study of free energy calculation and model reduction of stochastic dynamics [26, 30]. In order to construct processes which sample μ_1 or μ_2, we need to figure out the relations between the two surface measures ν_g and ν on Σ.

Lemma 2.2. *Let ν_g, ν be the surface measures on Σ induced from the metric $g = a^{-1}$ and the Euclidean metric on $\mathbb{R}^d$, respectively. We have*

$$\mathrm{d}\nu_g = (\det a)^{-\frac{1}{2}} \left[\frac{\det(\nabla\xi^T a \nabla\xi)}{\det(\nabla\xi^T\nabla\xi)}\right]^{\frac{1}{2}} \mathrm{d}\nu.$$

Proof. Let $x \in \Sigma$ and $\boldsymbol{v}_1, \boldsymbol{v}_2, \ldots, \boldsymbol{v}_{d-k}$ be a basis of $T_x\Sigma$. Assume that $\boldsymbol{v}_i = c_{ij}\boldsymbol{e}_j$, where $c = (c_{ij})$ is a $(d-k)\times d$ matrix whose rank is $d-k$. Using the fact $\langle \boldsymbol{v}_i, \mathrm{grad}^{\mathcal{M}}\xi_\alpha\rangle_g = 0$ for $1 \le i \le d-k$, $1 \le \alpha \le k$, we can deduce that $c\,\nabla\xi = 0$. Calculating the surface measures ν_g and ν under this basis, we obtain

$$\mathrm{d}\nu_g = \left[\frac{\det(ca^{-1}c^T)}{\det(cc^T)}\right]^{\frac{1}{2}} \mathrm{d}\nu. \tag{2.4}$$

To simplify the right hand side of (2.4), we use the following equality

$$\begin{pmatrix} c \\ \nabla\xi^T a \end{pmatrix} \begin{pmatrix} c^T & \nabla\xi \end{pmatrix} = \begin{pmatrix} cc^T & 0 \\ \nabla\xi^T a c^T & \nabla\xi^T a \nabla\xi \end{pmatrix} = \begin{pmatrix} ca^{-1} \\ \nabla\xi^T \end{pmatrix} a \begin{pmatrix} c^T & \nabla\xi \end{pmatrix}.$$

After computing the determinants of the last two matrices above, we obtain

$$\det(cc^T)\,\det(\nabla\xi^T a\nabla\xi) = (\det a)\,\det\left[\begin{pmatrix} ca^{-1} \\ \nabla\xi^T \end{pmatrix}\begin{pmatrix} c^T & \nabla\xi \end{pmatrix}\right] = (\det a)\ \det\begin{pmatrix} ca^{-1}c^T & ca^{-1}\nabla\xi \\ 0 & \nabla\xi^T\nabla\xi \end{pmatrix}.$$

The conclusion follows after we substitute the above relation into (2.4). □

Applying Lemma 2.2 and Proposition 2.1, we can obtain ergodic processes whose invariant measures are given in (2.3).

Theorem 2.3. *Let μ_1, μ_2 be the two probability measures on Σ defined in (2.3). Consider the dynamics X_s, Y_s on $\mathbb{R}^d$ which satisfy the Ito SDEs*

$$\mathrm{d}X_s^i = -(Pa)_{ij}\frac{\partial U}{\partial x_j}\,\mathrm{d}s + \frac{1}{\beta}\frac{\partial (Pa)_{ij}}{\partial x_j}\,\mathrm{d}s + \sqrt{2\beta^{-1}}\,P_{j,i}\,\mathrm{d}W_s^j, \tag{2.5}$$

and

$$\mathrm{d}Y_s^i = -(Pa)_{ij}\frac{\partial\left[U - \frac{1}{2\beta}\ln\det(\nabla\xi^T\nabla\xi)\right]}{\partial x_j}\,\mathrm{d}s + \frac{1}{\beta}\frac{\partial (Pa)_{ij}}{\partial x_j}\,\mathrm{d}s + \sqrt{2\beta^{-1}}\,P_{j,i}\,\mathrm{d}W_s^j, \tag{2.6}$$

for $1 \le i \le d$, where $\beta > 0$ and $W_s = (W_s^1, W_s^2, \ldots, W_s^d)^T$ is a d-dimensional Brownian motion. Suppose that $X_0, Y_0 \in \Sigma$, then $X_s, Y_s \in \Sigma$ almost surely for $s \ge 0$. Furthermore, the unique invariant probability measures of the dynamics X_s and Y_s are μ_1 and μ_2, respectively.

Proof. Applying Lemma 2.2, we can rewrite the probability measures μ_1, μ_2 as

$$\begin{aligned} \mathrm{d}\mu_1 &= \frac{1}{Z}\mathrm{e}^{-\beta U}\left[\det(\nabla\xi^T\nabla\xi)\right]^{-\frac{1}{2}}\,\mathrm{d}\nu = \frac{1}{Z}\exp\left[-\beta\left(U + \frac{1}{2\beta}\ln\frac{\det(\nabla\xi^T a\nabla\xi)}{\det a}\right)\right]\,\mathrm{d}\nu_g, \\ \mathrm{d}\mu_2 &= \frac{1}{Z}\mathrm{e}^{-\beta U}d\nu = \frac{1}{Z}\exp\left[-\beta\left(U + \frac{1}{2\beta}\ln\frac{\det\left(\nabla\xi^T a\nabla\xi\right)}{(\det a)\det(\nabla\xi^T\nabla\xi)}\right)\right]\,\mathrm{d}\nu_g, \end{aligned} \tag{2.7}$$

where again Z denotes different normalization constants. Applying Proposition 2.1 to the two probability measures expressed in (2.7), we can conclude that both the dynamics X_s in (2.5) and Y_s in (2.6) evolve on the submanifold Σ, and their invariant probability measures are given by μ_1 and μ_2, respectively. □

Remark 2.4. Under Assumptions 1.1 and 1.2, we can find a neighborhood $\mathcal{O}$ of Σ, such that P can be extended to $\mathcal{O}$. Furthermore, the relations in (A.9) are still satisfied in $\mathcal{O}$. Due to this fact, in (2.6) we can talk about the derivatives of P at states $x \in \Sigma$.

Remark 2.5. (1) Notice that, similar to (1.7), the infinitesimal generator of X_s in (2.5) can be written as

$$\mathcal{L} = \frac{\mathrm{e}^{\beta U}}{\beta} \frac{\partial}{\partial x_i} \left(\mathrm{e}^{-\beta U} (Pa)_{ij} \frac{\partial}{\partial x_j} \right). \tag{2.8}$$

Using (2.7) and (A.15), we can also verify the integration by parts formula

$$\int_\Sigma (\mathcal{L} f) f' \, \mathrm{d}\mu_1 = \int_\Sigma (\mathcal{L} f') f \, \mathrm{d}\mu_1 = -\frac{1}{\beta} \int_\Sigma (Pa \nabla f) \cdot \nabla f' \, \mathrm{d}\mu_1, \tag{2.9}$$

for any two C^2 smooth functions $f, f' : \Sigma \to \mathbb{R}$.

(2) Using Jacobi's formula [38] $\frac{\partial \ln \det(\nabla \xi^T \nabla \xi)}{\partial x_j} = (\nabla \xi^T \nabla \xi)^{-1}_{\alpha\eta} \frac{\partial (\nabla \xi_\alpha^T \nabla \xi_\eta)}{\partial x_j}$ and $(Pa)_{ij} \partial_j \xi_\alpha = 0$, the equation (2.6) can be simplified as

$$\mathrm{d}Y_s^i = -(Pa)_{ij} \frac{\partial U}{\partial x_j} \, \mathrm{d}s + \frac{1}{\beta} Q_{jl} \frac{\partial (Pa)_{ij}}{\partial x_l} \, \mathrm{d}s + \sqrt{2\beta^{-1}} \, P_{j,i} \, \mathrm{d}W_s^j,$$

where the matrix $Q = \mathrm{id} - \nabla \xi (\nabla \xi^T \nabla \xi)^{-1} \nabla \xi^T$. In the special case when $g = a = \mathrm{id}$, we have $\nu_g = \nu$ and $P_{j,i} = P_{ji} = Q_{ji}$ from (A.10). Accordingly, we can write the dynamics (2.6) as

$$\begin{aligned} \mathrm{d}Y_s^i &= -P_{ij} \frac{\partial U}{\partial x_j} \, \mathrm{d}s + \frac{1}{\beta} P_{lj} \frac{\partial P_{li}}{\partial x_j} \, \mathrm{d}s + \sqrt{2\beta^{-1}} \, P_{ji} \, \mathrm{d}W_s^j \\ &= -P_{ij} \frac{\partial U}{\partial x_j} \, \mathrm{d}s - \frac{1}{\beta} (\Psi^{-1})_{\alpha\gamma} P_{lj} (\partial_{lj}^2 \xi_\alpha) \partial_i \xi_\gamma \, \mathrm{d}s + \sqrt{2\beta^{-1}} \, P_{ji} \, \mathrm{d}W_s^j, \\ &= -P_{ij} \frac{\partial U}{\partial x_j} \, \mathrm{d}s + \frac{1}{\beta} H_i \, \mathrm{d}s + \sqrt{2\beta^{-1}} \, P_{ji} \, \mathrm{d}W_s^j, \end{aligned} \tag{2.10}$$

for $1 \le i \le d$, where $H = H_i \boldsymbol{e}_i$ is the mean curvature vector of Σ (see Prop. A.2). In Stratonovich form, (2.10) can be written as

$$\mathrm{d}Y_s^i = -P_{ij} \frac{\partial U}{\partial x_j} \, \mathrm{d}s + \sqrt{2\beta^{-1}} P_{ji} \circ \mathrm{d}W_s^j, \quad 1 \le i \le d. \tag{2.11}$$

In this case, our results are accordant with those in [10].

The dynamics constructed in Proposition 2.1 and Theorem 2.3 are reversible on Σ, in the sense that their infinitesimal generators are self-adjoint with respect to their invariant measures. In fact, using the same idea, we can construct non-reversible ergodic SDEs on Σ as well. We will only consider the conditional probability measure μ_1, since it is more relevant in applications and the result is also simpler.

Corollary 2.6. *Let μ_1 be the conditional probability measure on Σ defined in (2.3). The vector field $\boldsymbol{J} = (J_1, J_2, \ldots, J_d)^T = J_i \boldsymbol{e}_i$, defined on $x \in \Sigma$, satisfies*

$$\begin{aligned} \boldsymbol{J}(x) \in T_x \Sigma, \qquad & \forall \ x \in \Sigma, \\ P_{ij} \frac{\partial J_j}{\partial x_i} + J_j \frac{\partial P_{ij}}{\partial x_i} - \beta J_i \frac{\partial U}{\partial x_i} &= 0. \end{aligned} \tag{2.12}$$

Consider the dynamics X_s on $\mathbb{R}^d$ which satisfies the Ito SDE

$$\mathrm{d}X_s^i = J_i \, \mathrm{d}s - (Pa)_{ij} \frac{\partial U}{\partial x_j} \, \mathrm{d}s + \frac{1}{\beta} \frac{\partial (Pa)_{ij}}{\partial x_j} \, \mathrm{d}s + \sqrt{2\beta^{-1}} \, P_{j,i} \, \mathrm{d}W_s^j, \tag{2.13}$$

for $1 \le i \le d$, where $\beta > 0$ and $W_s = (W_s^1, W_s^2, \dots, W_s^d)^T$ is a d-dimensional Brownian motion. Suppose that $X_0 \in \Sigma$, then $X_s \in \Sigma$ almost surely for $s \ge 0$. Furthermore, the unique invariant probability measure of X_s is μ_1.

The proof can be found in Appendix A.

Remark 2.7. We make two remarks regarding the non-reversible vector $\boldsymbol{J}$.

(1) Notice that, as tangent vectors acting on functions, we have $P\boldsymbol{e}_j = P_{ij}\frac{\partial}{\partial x_i} \in T_x\Sigma$. Therefore, the condition (2.12) indeed only depends on the value of $\boldsymbol{J}$ on Σ. Supposing that $\boldsymbol{J}$ and U are defined in a neighborhood $\mathcal{O}$ of Σ (see Rem. 2.4), the condition (2.12) can be written equivalently as

$$\begin{aligned} &\boldsymbol{J}(x) \in T_x\Sigma, && \forall\, x \in \Sigma, \\ &\frac{\partial}{\partial x_i}\left[(P_{ij}J_j)\mathrm{e}^{-\beta U}\right] = 0, && \forall\, x \text{ near } \Sigma. \end{aligned} \tag{2.14}$$

(2) Recall that, the non-reversible dynamics on $\mathbb{R}^d$

$$\mathrm{d}\widetilde{Y}_s^i = \widetilde{J}_i(\widetilde{Y}_s)\,\mathrm{d}s - \left(a_{ij}\frac{\partial U}{\partial x_j}\right)(\widetilde{Y}_s)\,\mathrm{d}s + \frac{1}{\beta}\frac{\partial a_{ij}}{\partial x_j}(\widetilde{Y}_s)\,\mathrm{d}s + \sqrt{2\beta^{-1}}\sigma_{ij}(\widetilde{Y}_s)\,\mathrm{d}W_s^j, \quad 1 \le i \le d, \tag{2.15}$$

has the invariant probability density $\frac{1}{Z}\mathrm{e}^{-\beta U}$, if the vector $\widetilde{\boldsymbol{J}} = (\widetilde{J}_1, \widetilde{J}_2, \dots, \widetilde{J}_d)^T$ satisfies

$$\mathrm{div}(\widetilde{\boldsymbol{J}}\mathrm{e}^{-\beta U}) = \frac{\partial(\widetilde{J}_i\mathrm{e}^{-\beta U})}{\partial x_i} = 0, \qquad \forall\, x \in \mathbb{R}^d. \tag{2.16}$$

Comparing (2.16) with (2.14), it is clear that $\boldsymbol{J} = \widetilde{\boldsymbol{J}}|_\Sigma$ satisfies the condition (2.12) of Corollary 2.6 and can be used to construct non-reversible SDEs on Σ, provided that $P\widetilde{\boldsymbol{J}} = \widetilde{\boldsymbol{J}}$ in the neighborhood $\mathcal{O}$. Roughly speaking, in this case the vector field $\widetilde{\boldsymbol{J}}$ is tangential to the level sets of ξ in $\mathcal{O}$. In general cases, however, we can not simply take $\boldsymbol{J} = P\widetilde{\boldsymbol{J}}$ to obtain non-reversible processes on Σ which sample μ_1, since (2.14) may not be satisfied. We refer to Remark 3.8 in Section 3 for an alternative idea to develop "non-reversible" numerical schemes.

3. Numerical scheme sampling the conditional measure on Σ

Given a smooth function $f : \Sigma \to \mathbb{R}$ on the level set Σ, in this section we study the numerical scheme (1.11) and (1.12) in the Introduction, which allows us to numerically compute the average

$$\overline{f} = \int_\Sigma f(x)\,\mathrm{d}\mu_1(x) \tag{3.1}$$

with respect to the conditional probability measure μ_1 in (1.2).

To motivate the numerical scheme, let us first introduce the softly constrained dynamics, which satisfies the SDE

$$\mathrm{d}X_s^{\epsilon,i} = \left[-a_{ij}\frac{\partial U}{\partial x_j} - \frac{1}{\epsilon}a_{ij}\frac{\partial}{\partial x_j}\left(\frac{1}{2}\sum_{\alpha=1}^k \xi_\alpha^2\right) + \frac{1}{\beta}\frac{\partial a_{ij}}{\partial x_j}\right](X_s^\epsilon)\,\mathrm{d}s + \sqrt{2\beta^{-1}}\sigma_{ij}(X_s^\epsilon)\,\mathrm{d}W_s^j, \tag{3.2}$$

where $\epsilon > 0$, $1 \le i \le d$. It is straightforward to verify that (3.2) has a unique invariant measure

$$\mathrm{d}\mu^\epsilon(x) = \frac{1}{Z^\epsilon}\exp\left[-\beta\left(U(x) + \frac{1}{2\epsilon}\sum_{\alpha=1}^k \xi_\alpha^2(x)\right)\right]\mathrm{d}x, \quad \forall x \in \mathbb{R}^d, \tag{3.3}$$

where Z^ϵ is the normalization constant. As $\epsilon \to 0$, the authors in [10] studied the convergence of the dynamics (3.2) itself on a finite time horizon in the case when $a = \sigma = \mathrm{id}$ and $k = 1$. Closely related problems have also been studied in [13, 15, 22]. Since we are mainly interested in sampling the invariant measure, we record the following known convergence result of the measure μ^ϵ to μ_1. We omit its proof since it is a standard application of the co-area formula.

Lemma 3.1. *Let $f : \mathbb{R}^d \to \mathbb{R}$ be a bounded smooth function. μ_ϵ is the probability measure in (3.3) and μ_1 is the conditional probability measures on Σ defined in (2.3). We have*

$$\lim_{\epsilon \to 0} \int_{\mathbb{R}^d} f(x)\, \mathrm{d}\mu^\epsilon(x) = \frac{1}{Z} \int_\Sigma f(x) \mathrm{e}^{-\beta U(x)} \left[\det(\nabla \xi^T \nabla \xi)(x)\right]^{-\frac{1}{2}}\, \mathrm{d}\nu(x) = \int_\Sigma f(x)\, \mathrm{d}\mu_1(x),$$

where Z is the normalization constant given by

$$Z = \int_\Sigma \mathrm{e}^{-\beta U(x)} \left[\det(\nabla \xi^T \nabla \xi)(x)\right]^{-\frac{1}{2}}\, \mathrm{d}\nu(x).$$

Lemma 3.1 suggests that the softly constrained dynamics (3.2) with a small ϵ is a good candidate to sample μ_1 on Σ. However, direct simulation of (3.2) is probably inefficient when ϵ is small, because the time step-size in numerical simulations becomes limited due to the strong stiffness in the dynamics. The numerical scheme we will study below can be viewed as a multiscale numerical method for the dynamics (3.2). To explain the method, let us introduce the flow map $\varphi : \mathbb{R}^d \times [0, +\infty) \to \mathbb{R}^d$, defined by

$$\frac{\mathrm{d}\varphi(x,s)}{\mathrm{d}s} = -(a\nabla F)\big(\varphi(x,s)\big), \quad \varphi(x,0) = x, \qquad \forall\, x \in \mathbb{R}^d, \tag{3.4}$$

where the function F is

$$F(x) = \frac{1}{2}|\xi(x)|^2 = \frac{1}{2}\sum_{\alpha=1}^{k} \xi_\alpha^2(x). \tag{3.5}$$

Under proper conditions [13, 22], one can define the limiting map of φ as

$$\Theta(x) = \lim_{s \to +\infty} \varphi(x,s), \qquad \forall\, x \in \mathbb{R}^d. \tag{3.6}$$

Since $\nabla F|_\Sigma = 0$ and Σ is the set consisting of all global minima of F, it is clear that $\Theta : \mathbb{R}^d \to \Sigma$ and $\Theta(x) = x$, for $\forall\, x \in \Sigma$.

With the map Θ, we propose to approximate the average $\overline{f}$ in (3.1) by

$$\widehat{f}_n = \frac{1}{n}\sum_{l=0}^{n-1} f(x^{(l)}), \tag{3.7}$$

where n is a large number and the states $x^{(l)}$ are sampled from the numerical scheme

$$\begin{aligned} x_i^{(l+\frac{1}{2})} &= x_i^{(l)} + \left(-a_{ij}\frac{\partial U}{\partial x_j} + \frac{1}{\beta}\frac{\partial a_{ij}}{\partial x_j}\right) h + \sqrt{2\beta^{-1}h}\,\sigma_{ij}\eta_j^{(l)}, \quad 1 \le i \le d, \\ x^{(l+1)} &= \Theta\big(x^{(l+\frac{1}{2})}\big), \end{aligned} \tag{3.8}$$

starting from $x^{(0)} \in \Sigma$. In (3.8), $h > 0$ is the time step-size, functions a, σ, U are evaluated at $x^{(l)}$, and $\boldsymbol{\eta}^{(l)} = (\eta_1^{(l)}, \eta_2^{(l)}, \ldots, \eta_d^{(l)})^T$ are independent d-dimensional standard Gaussian random variables, for $0 \le l < n-1$.

Remark 3.2. We make two comments about the scheme (3.7) and (3.8).

(1) Since the image of Θ is on Σ, the discrete dynamics $x^{(l)}$ stays on Σ all the time. As in the case of the softly constrained dynamics (3.2), the numerical scheme has the advantage that only the 1st order derivatives of ξ are needed.
(2) When $a = \mathrm{id}$, the numerical scheme (3.8) becomes

$$\begin{aligned} x^{(l+\frac{1}{2})} &= x^{(l)} - \nabla U(x^{(l)})\, h + \sqrt{2\beta^{-1}h}\, \boldsymbol{\eta}^{(l)}, \\ x^{(l+1)} &= \Theta\big(x^{(l+\frac{1}{2})}\big). \end{aligned} \tag{3.9}$$

At each step $l \geq 0$, one needs to compute $\Theta(x^{(l+\frac{1}{2})})$. This can be done by solving the ODE (3.4) starting from $x^{(l+\frac{1}{2})}$, using numerical integration methods such as Runge–Kutta methods. In the following remark, we discuss issues associated with the computation of the ODE flow map Θ.

Remark 3.3 (Computation of the flow map Θ)**.**

(1) Exploiting the gradient structure of the ODE (3.4), we can in fact establish exponential convergence of the dynamics φ to its limit Θ, at least in the neighborhood $\mathcal{O}$ of Σ. For instance, we refer to [22] and Chapter 4 of [3]. Here, for brevity, we point out that the exponential decay of $F(\varphi(x,s))$ can be easily obtained and is therefore a good candidate for the convergence criterion in numerical implementations. Actually, under Assumptions 1.1 and 1.2, we can suppose

$$z^T \Psi(x) z \geq c_0 |z|^2, \quad \forall z \in \mathbb{R}^k, \quad \forall\, x \in \mathcal{O},$$

for some $c_0 > 0$, where $\Psi = \nabla \xi^T a \nabla \xi$. Direct calculation gives

$$\frac{\mathrm{d}F(\varphi(x,s))}{\mathrm{d}s} = -(\xi_\alpha \Psi_{\alpha\eta}\, \xi_\eta)(\varphi(x,s)) \leq -c_0 |\xi(\varphi(x,s))|^2 = -2c_0 F(\varphi(x,s)), \tag{3.10}$$

which implies that $|\xi(\varphi(x,s))|^2 = 2F(\varphi(x,s)) \leq \mathrm{e}^{-2c_0 s}|\xi(x)|^2$. In practice, suppose that we choose the condition $|\xi(\varphi(x,s))| \leq \epsilon_{\mathrm{tol}}$ as the stop criterion of ODE solvers and set $\Theta(x) = \varphi(x, s_{\mathrm{ode}})$ when the condition is met at the time s_{ode}. Then the above analysis indicates that we need to integrate the ODE (3.4) until the time $s_{\mathrm{ode}} = \max\big\{\frac{1}{c_0}\big(\ln|\xi(x^{(l+\frac{1}{2})})| + \ln\frac{1}{\epsilon_{\mathrm{tol}}}\big), 0\big\}$, which grows logarithmically as $\epsilon_{\mathrm{tol}} \to 0$. Since $x^{(l+\frac{1}{2})}$ is likely to remain close to Σ when h is small, we can expect that $\Theta(x^{(l+\frac{1}{2})})$ can be computed up to sufficient accuracy with affordable numerical effort.
(2) As a complement of the discussion above, we point out that adaptivity techniques (*e.g.*, using adaptive step-sizes) can be used to accelerate the computation of the flow map Θ. For instance, instead of (3.4), we can consider the ODE

$$\frac{\mathrm{d}\bar{\varphi}(x,s)}{\mathrm{d}s} = -(a\nabla|\xi|^{2-\kappa})\big(\bar{\varphi}(x,s)\big), \quad \bar{\varphi}(x,0) = x, \tag{3.11}$$

where $0 \leq \kappa < 1$. In fact, from the identity

$$\nabla|\xi|^{2-\kappa} = (2-\kappa)|\xi|^{-\kappa}\nabla\frac{|\xi|^2}{2} = (2-\kappa)\sum_{\alpha=1}^{k}\frac{\xi_\alpha}{|\xi|^\kappa}\nabla\xi_\alpha, \tag{3.12}$$

we know that ODE (3.11) is related to ODE (3.4) by a rescaling of the time s. Accordingly, for each x, the solution $\bar{\varphi}(x,\cdot)$ coincides with $\varphi(x,\cdot)$ after a reparametrization and therefore can be used to compute the projection $\Theta(x)$ as well. Furthermore, similar to (3.10), in this case we have

$$\frac{\mathrm{d}F(\bar{\varphi}(x,s))}{\mathrm{d}s} = -(2-\kappa)\left[|\xi|^{-\kappa}(\xi_\alpha \Psi_{\alpha\eta}\, \xi_\eta)\right](\bar{\varphi}(x,s)) \leq -c_0(2-\kappa)\left[2F(\bar{\varphi}(x,s))\right]^{1-\kappa/2},$$

from which we obtain $|\xi(\bar{\varphi}(x,s))|^\kappa \leq |\xi(x)|^\kappa - 2c_0(2-\kappa)s$, and therefore $\bar{\varphi}(x,s)$ reaches the state $\Theta(x) \in \Sigma$ before the finite time $s_{\mathrm{ode}} = \frac{|\xi(x)|^\kappa}{2c_0(2-\kappa)}$.

In applications, $\Theta(x)$ can be computed by solving the ODE (3.11) with a proper $\kappa \in [0,1)$ (and decreasing step-sizes). From the above discussion, in particular the identity (3.12), we know that this is equivalent to solving the ODE (3.4) using adaptive step-sizes. We refer to Examples 1 and 2 in Section 4 for numerical validation.

Our main result of this section concerns the approximation quality of the mean value $\overline{f}$ by the running average $\widehat{f}_n$ in (3.7), in the case when h is small and n is large. For this purpose, it is necessary to study the properties of the limiting flow map Θ, since it is involved in the numerical scheme (3.8). In fact, we have the following important result, which characterizes the derivatives of Θ by the projection map P in (1.9) (we refer the reader to (A.7)–(A.9) for properties of P).

Proposition 3.4. *Let Θ be the limiting flow map in (3.6) and P be the projection map in (1.9). At each $x \in \Sigma$, we have*

$$\begin{aligned} \frac{\partial \Theta_i}{\partial x_j} &= P_{ij}, \\ a_{lr}\frac{\partial^2 \Theta_i}{\partial x_l \partial x_r} &= \frac{\partial (Pa)_{il}}{\partial x_l} - P_{il}\frac{\partial a_{lr}}{\partial x_r}, \end{aligned} \tag{3.13}$$

for $1 \le i, j \le d$.

The proof of Proposition 3.4 can be found in Appendix B.

Based on the above result, we are ready to quantify the approximation error between the estimator $\widehat{f}_n$ and the mean value $\overline{f}$.

Theorem 3.5. *Suppose that both the step-size h and the number of the total steps n are fixed. Assume that $f : \Sigma \to \mathbb{R}$ is a smooth function on Σ and $\overline{f}$ is its mean value defined in (3.1) with respect to the measure μ_1. Consider the running average $\widehat{f}_n$ in (3.7), which is computed by simulating the numerical scheme (3.8) with time step-size $h > 0$. Let $T = nh$ and C denote a generic positive constant that is independent of h, n. We have the following approximation results.*

(1) $\left|\mathbf{E}\widehat{f}_n - \overline{f}\right| \le C(h + \frac{1}{T})$.
(2) $\mathbf{E}\left|\widehat{f}_n - \overline{f}\right|^2 \le C(h^2 + \frac{1}{T})$.
(3) *For any $0 < \epsilon < \frac{1}{2}$, there is an almost surely bounded positive random variable $\zeta(\omega)$, such that $|\widehat{f}_n - \overline{f}| \le Ch + \frac{\zeta(\omega)}{T^{1/2-\epsilon}}$, almost surely.*

We present the proof of Theorem 3.5 in Appendix B, since it is technical and the idea follows the standard approach developed in [35], where Poisson equation played a crucial role. However, let us emphasize that, in contrast to [35], in the current setting we are working on the submanifold Σ and, furthermore, the map Θ is involved in our numerical scheme. In particular, in the proof we use the Poisson equation related to the generator $\mathcal{L}$ in (1.10) of the process (1.8), based on the fact that μ_1 is the invariant measure of (1.8) (This is the place where Thm. 2.3 in Sect. 2 is used in order to establish Thm. 3.5).

Remark 3.6. Theorem 3.5 concerns the long time behavior of the scheme (3.8) with a small step-size, *i.e.*, large T and small h. This is often relevant in molecular dynamics simulations. While the estimates of Theorem 3.5 are stated in terms of the variables h and T, we should point out that the time $T = nh$ and therefore it depends on both h and n. Alternatively (and more precisely), the estimates can be expressed using the independent variables h and n. For instance, for the mean square error estimate, we have

$$\mathbf{E}\left|\widehat{f}_n - \overline{f}\right|^2 \le C\left(h^2 + \frac{1}{nh}\right). \tag{3.14}$$

Therefore, for a fixed (large) total sample number n, we can conclude that the optimal upper bound in (3.14) is $\mathcal{O}(n^{-\frac{2}{3}})$ and is achieved when $h = \mathcal{O}(n^{-\frac{1}{3}})$. We refer to [35] for related discussions.

In applications, the conditional probability measure μ_1 often satisfies the following Poincaré inequality [29]

$$\mathrm{Var}_{\mu_1}(f) := \int_\Sigma (f-\overline{f})^2 \,\mathrm{d}\mu_1 \le -\frac{1}{K}\int_\Sigma (\mathcal{L}f) f \,\mathrm{d}\mu_1 = \frac{1}{K\beta}\int_\Sigma (Pa\nabla f)\cdot\nabla f \,\mathrm{d}\mu_1, \tag{3.15}$$

for all $f:\Sigma\to\mathbb{R}$ such that the right hand side of the above inequality is finite, where $K>0$ is the Poincaré constant, $\mathcal{L}$ is the infinitesimal generator (1.10), and the identity (2.9) in Remark 2.5 has been used. Under this condition, the mean square error estimate in Theorem 3.5 can be improved (*i.e.*, the constant in front of the $\mathcal{O}(T^{-1})$ term is small when K is large) and we have the following corollary (The proof is in Appendix B).

Corollary 3.7. *Under the same assumptions in Theorem 3.5 and further assuming that μ_1 satisfies the Poincaré inequality (3.15), we have*

$$\mathbf{E}\big|\widehat{f}_n - \overline{f}\big|^2 \le \frac{2C_1\mathrm{Var}_{\mu_1}(f)}{KT} + C_2\left(h^2+\frac{h}{T}+\frac{1}{T^2}\right),$$

where C_1 is any constant larger than 1, the constant C_2 depends on the choice of C_1 but is independent of both h and n.

Remark 3.8 (Non-reversible schemes)**.** The idea of using the map Θ in the constraint step of the numerical scheme (3.8) is motivated by the softly constrained (reversible) dynamics (3.2). It is natural to consider whether certain "non-reversible" numerical scheme can be obtained using the same idea. In fact, let $A\in\mathbb{R}^{d\times d}$ be a constant skew-symmetric matrix such that $A^T=-A$. The softly constrained (non-reversible) dynamics

$$\begin{aligned}\mathrm{d}X_s^{\epsilon,A,i} = &\left[A_{ij}\frac{\partial}{\partial x_j}\left(U+\frac{1}{2\epsilon}\sum_{\alpha=1}^k \xi_\alpha^2\right) - a_{ij}\frac{\partial U}{\partial x_j} - \frac{1}{\epsilon}a_{ij}\frac{\partial}{\partial x_j}\left(\frac{1}{2}\sum_{\alpha=1}^k\xi_\alpha^2\right) + \frac{1}{\beta}\frac{\partial a_{ij}}{\partial x_j}\right](X_s^{\epsilon,A})\,\mathrm{d}s\\ &+\sqrt{2\beta^{-1}}\sigma_{ij}(X_s^{\epsilon,A})\,\mathrm{d}W_s^j,\end{aligned} \tag{3.16}$$

indeed has the same invariant measure μ^ϵ in (3.3). Based on this fact, a reasonable guess of the "non-reversible" numerical scheme that samples the conditional measure μ_1 is the multiscale method of (3.16), *i.e.*,

$$\begin{aligned} x_i^{(l+\frac{1}{2})} &= x_i^{(l)} + \left(A_{ij}\frac{\partial U}{\partial x_j} - a_{ij}\frac{\partial U}{\partial x_j} + \frac{1}{\beta}\frac{\partial a_{ij}}{\partial x_j}\right)(x^{(l)})\,h + \sqrt{2\beta^{-1}h}\,\sigma_{ij}(x^{(l)})\,\eta_j^{(l)}, \quad 1\le i\le d,\\ x^{(l+1)} &= \Theta^A\big(x^{(l+\frac{1}{2})}\big),\end{aligned} \tag{3.17}$$

where $\Theta^A(x)=\lim\limits_{s\to+\infty}\varphi^A(x,s)$ is the limit of the (non-gradient) flow map

$$\frac{\mathrm{d}\varphi^A(x,s)}{\mathrm{d}s} = -((a-A)\nabla F)\big(\varphi^A(x,s)\big), \quad \varphi^A(x,0)=x, \qquad \forall\, x\in\mathbb{R}^d, \tag{3.18}$$

with the same function F in (3.5). We expect that the long time sampling error estimates of the numerical scheme (3.17) can be studied following the same approach of this section as well. For this purpose, however, it is necessary to handle the non-gradient term in the ODE (3.18), which brings difficulties when calculating the derivatives of the map Θ^A (*cf.*, Prop. 3.4 as well as its proof in Appendix B). We will postpone the analysis in the future work and readers are referred to Example 1 in Section 4 for numerical validation of the scheme (3.17 and (3.18).

In the literature, reversible Metropolis random walk on submanifold [43] and Hybrid Monte Carlo algorithm [32] have been proposed to sample distributions on submanifolds. A comprehensive comparison between our scheme (without Metropolis step) and these Metropolis-adjusted approaches is a complicate task and goes beyond the scope of the current paper. We only discuss this issue briefly in the following remark.

Remark 3.9 (Comparison to the Metropolis-adjusted samplers [32, 43] on submanifolds)**.** We compare the following three aspects.

(1) *Constraint step.* In the scheme (3.8), the map Θ in (3.6) is used to project the state $x^{(l+\frac{1}{2})}$ to the submanifold Σ. Under mild assumptions, the gradient structure of the ODE (3.4) allows to define Θ for all states at which the map ξ is C^2 smooth (Assumption 1.2). Differently, in [32,43], newly proposed states are projected back to the submanifold by solving a nonlinear system. One usually uses Newton's method to find the solution of the system, with the hope that the convergence can be achieved within a few iteration steps (success), thanks to the quadratic convergence rate of Newton's method. In practice, however, it may happen that either the solution does not exist or, even if the solution exists, the Newton's method does not converge (due to local convergence). In these two cases, the constraint step ends without finding a new state on the submanifold (no success). Although the Markov chain samples the correct invariant distribution regardless whether the constraint step is successful or not [43], the sampling efficiency is affected by the success rate of the constraint step.

(2) *Computational complexity.* Suppose the computational complexity of evaluating the $d\times k$ matrix $\nabla\xi$ is $\mathcal{O}(k\cdot d)$ and n states are sampled in total. In each step of both the scheme (3.8) and the Metropolis-adjusted methods in [32, 43], the major computational effort is devoted to the constraint step, *i.e.*, either computing the map Θ by integrating ODE or solving equations using Newton's method. For the scheme (3.8) with $a = \mathrm{id}$, the overall computational complexity of the constraint step is therefore $\mathcal{O}(n \cdot k \cdot d \cdot s_{\mathrm{ode}}/\Delta s)$, where s_{ode} and Δs are the average final time (see Rem. 3.3) and the average step-size in the ODE integration, respectively. For the Metropolis-adjusted methods in [32, 43], in each Newton iteration it is necessary to compute the matrix product $\nabla\xi^T(x)\nabla\xi(x')$ for two states x, x'. Therefore, the overall computational complexity is $\mathcal{O}(n \cdot k^2 \cdot d \cdot N_{\mathrm{iter}})$, where N_{iter} is the average total iteration steps of Newton's method. In practice, one can implement the method in [43] in a way such that Newton's method ends within a few Newton iterations, *e.g.*, $N_{\mathrm{iter}} \leq 10$. On the other hand, the ODE integration in the scheme (3.8) requires more iteration steps (for the examples in Section 4, 20–40 steps are needed), *i.e.*, $s_{\mathrm{ode}}/\Delta s \geq N_{\mathrm{iter}}$. However, when comparing the computational cost of both methods, we should keep in mind that an ODE iteration step is generally cheaper than a Newton iteration step, since the latter involves both matrix-matrix multiplication and solving linear systems (the cost of solving $k \times k$ linear systems is not major and therefore for simplicity is not included in the estimation above). While the computational cost of Newton's method is smaller when k is small, the ODE integration becomes faster for medium or large k. We refer to Example 2 in Section 4 for numerical comparison on the computational cost of both methods.

(3) *Choice of step-size.* To apply the scheme (3.8), one usually chooses a suitably small step-size h and runs the scheme for sufficient many steps (large n). In concrete applications, one often needs to tune the step-size h, keeping in mind that a large h will lead to large bias, while a unnecessarily small h will result in large correlations. See Remark 3.6. For the Metropolis-adjusted methods [32,43], the choice of the step-size (in the proposal step) is in fact a more delicate issue. Although the Markov chain remains unbiased for large step-sizes, the sampling efficiency will be possibly limited due to a low acceptance rate in the Metropolis step. This issue has been discussed in [32], where the performance with different step-sizes has been numerically investigated. Besides the acceptance rate in the Metropolis step, the success rate of the constraint step also depends on the step-size used in the proposal step. Taking the $(d-1)$-dimensional unit sphere $\mathbb{S}^{d-1}$ as an example, it is not difficult to see that there won't be corresponding projected state on the sphere (*i.e.*, the solution of the constraint equation does not exist), if the norm of the tangent vector generated in the proposal step (see [43]) is larger than one. This implies that the success rate of the constraint step will decrease when we increase the step-size in the proposal step. To summarize, it is important to choose the step-size in the Metropolis-adjusted method in [32, 43] properly, such that both the acceptance rate in the Metropolis step and the success rate of the constraint step are not too small.

Before concluding, let us point out that the approach used in the above proof allows us to study other numerical schemes on Σ as well. As an example, we consider the projection from $\mathbb{R}^d$ to Σ along geodesic

curves (instead of using the flow map (3.4)–(3.6)) defined by the metric $g = a^{-1}$ in (1.13), *i.e.*, the metric on $\mathcal{M} = (\mathbb{R}^d, g)$. Let d be the distance function on $\mathbb{R}^d$ induced by the metric g in (1.13). We introduce the projection function

$$\Pi(x) = \left\{ y \,\middle|\, d(x,y) = d(x,\Sigma),\, y \in \Sigma \right\}, \quad \forall\, x \in \mathbb{R}^d. \tag{3.19}$$

Clearly, we have $\Pi|_\Sigma = \mathrm{id}|_\Sigma$. Given any $x \in \Sigma$, there is a neighborhood $\Omega \subset \mathbb{R}^d$ of x such that $\Pi|_\Omega$ is a single-valued map. Furthermore, applying inverse function theorem, we can verify that Π is smooth on Ω. Similar to Proposition 3.4, we need the following result which connects the derivatives of Π to the projection map P in (1.9) (note that, comparing to the derivatives of the map Θ in (3.13), there is an extra term in the second equation of (3.20)). Its proof is given in Appendix B.

Proposition 3.10. *Let $\Pi = (\Pi_1, \Pi_2, \dots, \Pi_d)^T : \mathbb{R}^d \to \Sigma$ be the projection function in (3.19), where $\Pi_i : \mathbb{R}^d \to \mathbb{R}$ are smooth functions, $1 \le i \le d$. For $x \in \Sigma \cap \Omega$, we have*

$$\begin{aligned} \frac{\partial \Pi_i}{\partial x_j} &= P_{ij}, \\ a_{lr}\frac{\partial^2 \Pi_i}{\partial x_l \partial x_r} &= -P_{il}\frac{\partial a_{lr}}{\partial x_r} + \frac{\partial (Pa)_{il}}{\partial x_l} + \frac{1}{2}(Pa)_{il}\frac{\partial \ln \det \Psi}{\partial x_l}, \end{aligned} \tag{3.20}$$

for $1 \le i, j \le d$, where $\Psi = \nabla \xi^T a \nabla \xi$.

Now we are ready to study the numerical scheme

$$\begin{aligned} x_i^{(l+\frac{1}{2})} &= x_i^{(l)} + \left(-a_{ij}\frac{\partial U}{\partial x_j} + \frac{1}{\beta}\frac{\partial a_{ij}}{\partial x_j} \right)(x^{(l)})\, h + \sqrt{2\beta^{-1}h}\, \sigma_{ij}(x^{(l)})\, \eta_j^{(l)}, \quad 1 \le i \le d, \\ x^{(l+1)} &= \Pi\big(x^{(l+\frac{1}{2})}\big), \end{aligned} \tag{3.21}$$

where $x^{(0)} \in \Sigma$, and the map Π (instead of Θ) is used in each step to project the states $x^{(l+\frac{1}{2})}$ back to Σ.

Theorem 3.11. *Assume that $f : \Sigma \to \mathbb{R}$ is a smooth function on Σ and $\overline{\overline{f}}$ is its mean value*

$$\overline{\overline{f}} = \int_\Sigma f(x)\, \mathrm{d}\mu(x),$$

with respect to the probability measure

$$\mathrm{d}\mu = \frac{1}{Z}\mathrm{e}^{-\beta U}\sqrt{\frac{\det(\nabla \xi^T a \nabla \xi)}{\det(\nabla \xi^T \nabla \xi)}}\, \mathrm{d}\nu. \tag{3.22}$$

Consider the running average $\widehat{f}_n$ in (3.7), which is computed by simulating the numerical scheme (3.21) with time step-size $h > 0$. Let $T = nh$ and C denote a generic positive constant that is independent of h, T. We have the following approximation results.

(1) $\left|\mathbf{E}\widehat{f}_n - \overline{\overline{f}}\right| \le C(h + \frac{1}{T})$.
(2) $\mathbf{E}\left|\widehat{f}_n - \overline{\overline{f}}\right|^2 \le C(h^2 + \frac{1}{T})$.
(3) *For any $0 < \epsilon < \frac{1}{2}$, there is an almost surely bounded positive random variable $\zeta(\omega)$, such that $|\widehat{f}_n - \overline{\overline{f}}| \le Ch + \frac{\zeta(\omega)}{T^{1/2-\epsilon}}$, almost surely.*

We omit the proof since it resembles the proof of Theorem 3.5.

Remark 3.12. For the projection map Π induced by a general metric $g = a^{-1}$ or, equivalently, by a general (positive definite) matrix a, implementing the numerical scheme (3.21) is not as easy as the numerical scheme (3.8). We decide to omit the algorithmic discussions, due to the fact that the probability measure (3.22) seems less relevant in applications. However, it is meaningful to point out that, when $a = \mathrm{id}$, the above result is relevant to the one in [10]. In this case, the probability measure in (3.22) reduces to $\mu_2 = \frac{1}{Z}\mathrm{e}^{-\beta U}\,\mathrm{d}\nu$ in (2.3) and the numerical scheme (3.21) can be formulated equivalently using Lagrange multiplier. We refer to [10,31] for comprehensive numerical details.

4. Numerical examples

In this section, we study three concrete examples. In the first example, we investigate the different schemes in Section 3. In particular, the sampling performance of the constrained schemes using different maps Θ, Θ^A, and Π, as well as the performance of the unconstrained Euler–Maruyama discretization of the SDE (2.5), will be compared. In the second example, we compare the computational costs of the scheme (3.8) and the Metropolis-adjusted algorithm introduced in [43]. In the last example, we show that in some cases it is helpful to consider non-constant matrices σ and a. The C/C++ code used for producing the numerical results in the following examples is available at: https://github.com/zwpku/sampling-on-levelset.

Example 1: Comparison of schemes using different projection maps

Let us define $\xi : \mathbb{R}^2 \to \mathbb{R}$ by

$$\xi(x) = \frac{1}{2}\left(\frac{x_1^2}{c^2} + x_2^2 - 1\right), \quad \forall\, x = (x_1, x_2)^T \in \mathbb{R}^2,$$

with the constant $c = 3$. The level set $\Sigma = \left\{(x_1, x_2)^T \mid \frac{x_1^2}{c^2} + x_2^2 = 1\right\}$ is an ellipse in $\mathbb{R}^2$. We have $\nabla\xi = (\frac{x_1}{c^2}, x_2)^T$ and therefore $\det(\nabla\xi^T\nabla\xi) = |\nabla\xi|^2 = \frac{x_1^2}{c^4} + x_2^2$. For simplicity, we choose the potential $U = 0$ and the matrices $a = \sigma = \mathrm{id} \in \mathbb{R}^{2\times 2}$. The two probability measures in (2.3) on Σ are

$$\mathrm{d}\mu_1 = \frac{1}{Z}\left(\frac{x_1^2}{c^4} + x_2^2\right)^{-\frac{1}{2}} \mathrm{d}\nu, \quad \mathrm{d}\mu_2 = \frac{1}{Z}\,\mathrm{d}\nu,$$

where Z denotes two different normalization constants and ν is the surface measure on Σ. Since Σ is a one-dimensional manifold, it is helpful to consider the parametrization of Σ by

$$x_1 = c\cos\theta, \quad x_2 = \sin\theta, \tag{4.1}$$

where the angle $\theta \in [0, 2\pi]$. Applying the chain rule $\frac{\partial}{\partial\theta} = -c\sin\theta\frac{\partial}{\partial x_1} + \cos\theta\frac{\partial}{\partial x_2}$, we can obtain the expressions of μ_1, μ_2 under this coordinate as

$$\mathrm{d}\mu_1 = \frac{1}{Z}\mathrm{d}\theta, \quad \mathrm{d}\mu_2 = \frac{1}{Z}\left(c^2\sin^2\theta + \cos^2\theta\right)^{\frac{1}{2}}\mathrm{d}\theta. \tag{4.2}$$

With these preparations, we proceed to study the following four numerical approaches.

(1) *Numerical scheme (3.8) using* Θ. Since $U \equiv 0$ and $a = \mathrm{id}$, (3.8) becomes

$$\begin{aligned} x^{(l+\frac{1}{2})} &= x^{(l)} + \sqrt{2\beta^{-1}h}\,\boldsymbol{\eta}^{(l)}, \\ x^{(l+1)} &= \Theta\left(x^{(l+\frac{1}{2})}\right), \end{aligned} \tag{4.3}$$

where $\Theta(x)$ is the limit of the flow map φ, given by

$$\dot{y}_1(s) = -\frac{\xi\left(y(s)\right)y_1(s)}{c^2}, \quad \dot{y}_2(s) = -\xi(y(s))\,y_2(s), \qquad s \geq 0, \tag{4.4}$$

starting from $y(0) = x$.

(2) *Numerical scheme (3.17) and (3.18) using* Θ^A. Let us choose the skew-symmetric matrix

$$A = \begin{pmatrix} 0 & 1/2 \\ -1/2 & 0 \end{pmatrix}. \tag{4.5}$$

Since $U \equiv 0$ and $a = \mathrm{id}$, we have

$$\begin{aligned} x^{(l+\frac{1}{2})} &= x^{(l)} + \sqrt{2\beta^{-1}h}\,\boldsymbol{\eta}^{(l)}, \\ x^{(l+1)} &= \Theta^A\big(x^{(l+\frac{1}{2})}\big), \end{aligned} \tag{4.6}$$

where $\Theta^A(x)$ is the limit of the flow map φ^A, given by

$$\dot{y}_1(s) = -\xi\big(y(s)\big)\left(\frac{y_1(s)}{c^2} - \frac{y_2(s)}{2}\right), \quad \dot{y}_2(s) = -\xi\big(y(s)\big)\left(\frac{y_1(s)}{2c^2} + y_2(s)\right), \qquad s \geq 0, \tag{4.7}$$

starting from $y(0) = x$.

(3) *Numerical scheme (3.21) using* Π. Similarly, since $U \equiv 0$ and $a = \mathrm{id}$, (3.21) becomes

$$\begin{aligned} x^{(l+\frac{1}{2})} &= x^{(l)} + \sqrt{2\beta^{-1}h}\,\boldsymbol{\eta}^{(l)}, \\ x^{(l+1)} &= \Pi\big(x^{(l+\frac{1}{2})}\big), \end{aligned} \tag{4.8}$$

where Π is the projection map onto Σ, defined in (3.19).

(4) *Euler–Maruyama discretization of the SDE (2.5).* Notice that we have $Pa = P$, and it is straightforward to compute

$$P_{11} = \frac{c^4x_2^2}{x_1^2 + c^4x_2^2}, \quad P_{12} = P_{21} = -\frac{c^2x_1x_2}{x_1^2 + c^4x_2^2}, \quad P_{22} = \frac{x_1^2}{x_1^2 + c^4x_2^2}.$$

Therefore, discretizing (2.5), we obtain

$$\begin{aligned} x_1^{(l+1)} &= x_1^{(l)} + \frac{1}{\beta}\frac{c^4(c^2-2)x_1x_2^2 - c^2x_1^3}{(x_1^2 + c^4x_2^2)^2}\,h + \sqrt{2\beta^{-1}h}\left(\frac{c^4x_2^2}{x_1^2 + c^4x_2^2}\,\eta_1^{(l)} - \frac{c^2x_1x_2}{x_1^2 + c^4x_2^2}\,\eta_2^{(l)}\right) \\ x_2^{(l+1)} &= x_2^{(l)} + \frac{1}{\beta}\frac{(1-2c^2)x_1^2x_2 - c^6x_2^3}{(x_1^2 + c^4x_2^2)^2}\,h + \sqrt{2\beta^{-1}h}\left(-\frac{c^2x_1x_2}{x_1^2 + c^4x_2^2}\,\eta_1^{(l)} + \frac{x_1^2}{x_1^2 + c^4x_2^2}\,\eta_2^{(l)}\right). \end{aligned} \tag{4.9}$$

Based on Theorems 2.3, 3.11, and Remark 3.8, we study the performance of the schemes (4.3), (4.6), and (4.9) in sampling the conditional measure μ_1, as well as the performance of the scheme (4.8) in sampling the measure μ_2.

In the numerical experiment, we choose $\beta = 1.0$ in each of the above schemes. For the first scheme using Θ, we simulate (4.3) for $n = 2 \times 10^7$ steps with the step-size $h = 0.01$. In each constraint step, $\Theta(x^{(l+\frac{1}{2})})$ is computed by solving the ODE (4.4) starting from $y(0) = x^{(l+\frac{1}{2})}$ until the time when $|\xi(y(s))| < 10^{-8}$ is satisfied, using the 3rd order (Bogacki–Shampine) Runge–Kutta (RK) method. The adaptivity technique in the second point of Remark 3.3 is used with $\kappa = 0.5$. The step-size for solving the ODE is set to $\Delta s = 0.1$ initially and is divided by 2.0 whenever we find that the value of $|\xi|$ is not decreasing (the numerical error of Θ is 3.7×10^{-7} on average, comparing to the reference solution that is obtained by solving the ODE with $\kappa = 0$ and the fixed step-size $\Delta s = 0.001$). On average, we observe that 25 iterations of the RK method are needed in each constraint step in order to meet the criterion $|\xi(y(s))| < 10^{-8}$.

For the second scheme using Θ^A, we simulate (4.6) for $n = 2 \times 10^7$ steps with the step-size $h = 0.005$. Notice that, a slightly smaller step-size h is used, because in this case the non-gradient ODE flow (4.7) produces a drift force on the level set Σ. In each constraint step, $\Theta^A(x^{(l+\frac{1}{2})})$ is computed by solving the ODE (4.7) in the same way (with the same parameters) as we did in the first scheme. On average, we find that 23 iterations of the RK method are needed in each constraint step in order to meet the criterion $|\xi(y(s))| < 10^{-8}$.

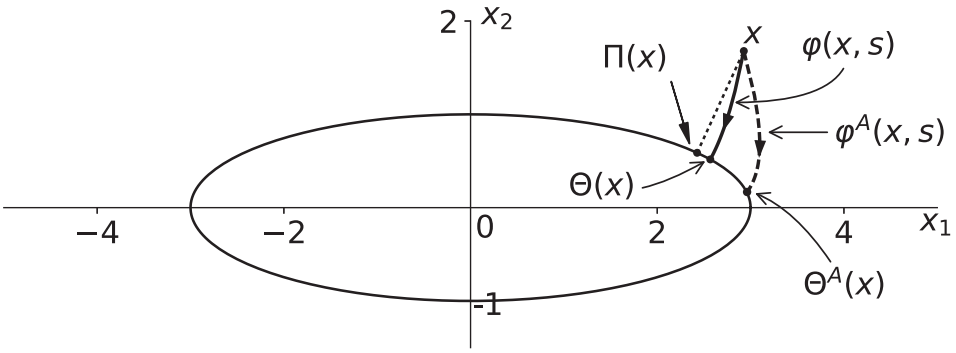

FIGURE 1. Example 1. Given $x \in \mathbb{R}^2$, $\Pi(x)$ is the state on the ellipse Σ which achieves the minimal distance to x, while $\Theta(x)$ and $\Theta^A(x)$ are the limits of the ODE flows (4.4) and (4.7) starting from x, respectively.

For the third scheme using Π, (4.8) is simulated for $n = 2 \times 10^7$ steps with the step-size $h = 0.01$. Using the parametrization (4.1), we have $\Pi(x) = (c\cos\theta^*, \sin\theta^*)^T$, where

$$\theta^* = \underset{\theta\in[0,2\pi]}{\arg\min} \left((x_1 - c\cos\theta)^2 + (x_2 - \sin\theta)^2\right), \quad x = (x_1, x_2)^T. \tag{4.10}$$

Therefore, in each step, $\Pi(x^{(l+\frac{1}{2})})$ is computed by solving (4.10) using the simple gradient descent method. The step-size is fixed to $\Delta t = 0.1$ and the gradient descent iteration terminates when the derivative of the objective function in (4.10) has an absolute value that is less than 10^{-8}. On average, it requires 32 gradient descent iterations in each step in order to meet the convergence criterion.

Let us make a comparison among the three schemes (4.3), (4.6) and (4.8). From Figures 1 and 2, we can see that the three maps Θ, Θ^A and Π indeed have different effects. Roughly speaking, comparing to the projection map Π, both Θ and Θ^A tend to map states towards one of the two vertices $(\pm c, 0)$, where $|\nabla\xi|$ are smaller, while Π^A introduces a further rotational force on Σ. Based on the states generated from these three schemes, in Figure 3 we show the empirical probability densities of the parameter θ in (4.1). From the agreement between the empirical densities and the densities computed from the analytical expressions in (4.2), we can make the conclusion that the trajectories generated from the two schemes using Θ and Θ^A indeed sample the probability measure μ_1, while the trajectory generated from the scheme using Π samples μ_2.

Lastly, concerning the fourth scheme, we simulate (4.9) for $n = 10^7$ steps using the step-size $h = 0.0001$. In this case, we find that it is necessary to choose a small step-size h in order to keep the trajectory close to the level set Σ. As can be seen from Figure 4, even with this smaller step-size $h = 0.0001$, the generated trajectory departs from the level set Σ. This indicates the limited usefulness of the direct Euler–Maruyama discretization of the SDE (2.5) in long time simulations.

Example 2: Numerical comparison with the Metropolis-adjusted method on the special orthogonal group SO(11).

In this example, we compare the computational efficiency between our scheme (3.8) using the flow map Θ and the Metropolis-adjusted method introduced in [43]. We consider the special orthogonal group SO(11), which consists of orthogonal matrices of size 11×11 with determinant equals to 1. This example is taken from [43]. The authors there applied their method to the estimation of the mean value of the function $f(x) = \mathrm{Tr}(x)$, *i.e.*, the trace of the matrix x, where x follows the surface measure of SO(11). The manifold SO(11) can be viewed as (one connected component of) the level set of the map $\xi : \mathbb{R}^{121} \to \mathbb{R}^{66}$, which includes all the row ortho-normality constraints. Readers are referred to the original work [43] for a detailed introduction on the example.

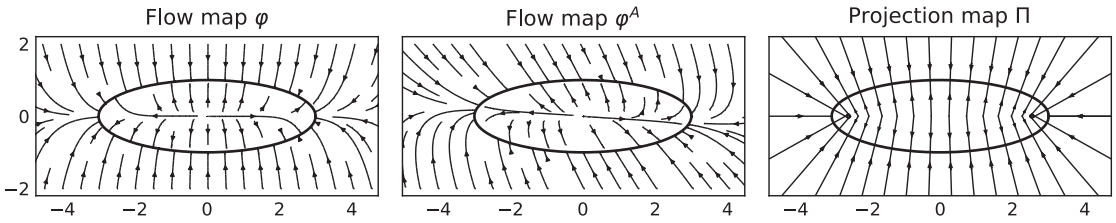

FIGURE 2. Example 1. Left: the streamline of the flow map φ in (4.4). Middle: the streamline of the flow map φ^A (4.7) with the matrix A in (4.5). Right: illustration of the projection Π. Points on each straight line are mapped to the same point on Σ.

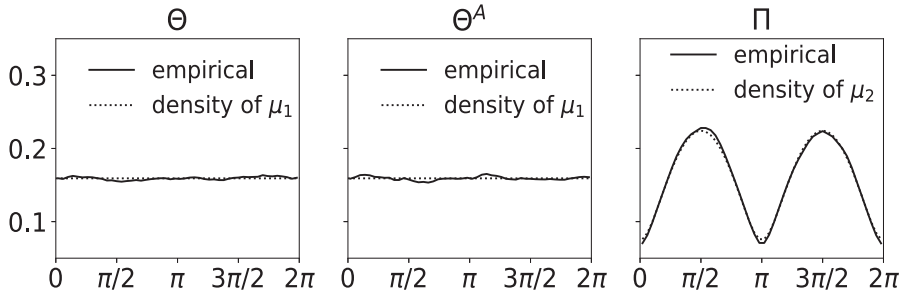

FIGURE 3. Example 1. The probability densities of the parameter θ, computed from the scheme (4.3) using Θ (left plot), the scheme (4.6) using Θ^A (middle plot), and the scheme (4.8) using Π (right plot). In each plot, dotted curves are the probability densities computed from the analytical expressions of μ_1, μ_2 in (4.2), respectively. Solid lines are the empirical probability densities of θ estimated using the states generated from the schemes (4.3), (4.6) and (4.8), respectively.

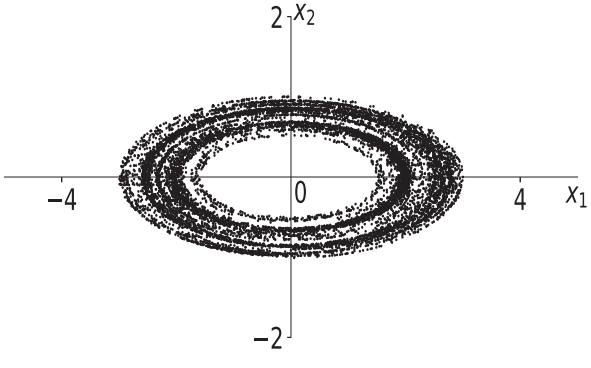

FIGURE 4. Example 1. States generated from the Euler–Maruyama discretization (4.9), where we choose $h = 0.0001$ and $n = 10^7$. In this case, the sampled states deviate from the level set Σ.

In this numerical study, we implement both the scheme (3.8) and the (Metropolis-adjusted) algorithm in [43] to estimate the mean value of $\mathrm{Tr}(x)$. Notice that, since $\det(\nabla\xi^T\nabla\xi)$ is constant, the conditional measure μ_1 in (1.2) coincides with the surface measure of SO(11) when we choose the potential $U \equiv 0$. In both cases, we generate $n = 10^6$ samples on the same laptop (CPU: Intel Core i5, 2.60 GHz, 4 cores; system: Ubuntu 18.04). For the scheme (3.8), we choose the step-size $h = 0.022$. The map Θ is computed by integrating the ODE (3.4) with $a = \mathrm{id}$, until the condition $|\xi(\varphi(x,s))| < 10^{-9}$ is satisfied. To accelerate the ODE integration, we have applied the adaptivity technique in the second point of Remark 3.3 with $\kappa = 0.5$. Starting from the initial step-size $\Delta s = 0.2$, the step-size used in the ODE integration is divided by 2.0 whenever we find that the value of $|\xi|$ is not decreasing (the numerical error of Θ is 2.0×10^{-4} on average, comparing to the reference solution that is obtained by solving the ODE with $\kappa = 0$ and the fixed step-size $\Delta s = 0.002$). Furthermore, the new state will be discarded (and resampled) if its determinant equals to -1. With these parameters, we observe that on average 37 Runge–Kutta iterations are needed for each evaluation of the map Θ. In total, it takes 2676.9 s to generate $n = 10^6$ samples, while the estimated mean value of $\mathrm{Tr}(x)$ is 3.8×10^{-3} with a statistical error 3.9×10^{-3}. For the algorithm in [43], the maximal number of Newton steps is set to 10 and the proposal length scale is chosen to be 0.257^2. In our experiment, we find that this proposal length scale (different from the one used in [43]) leads to slightly smaller correlation time. Within the entire computation, the success rate of the Newton's method (*i.e.*, the rate that the Newton's method converges) is 67.2 each time it takes 5–6 iterations on average for the Newton's method to reach convergence (the convergence criteria is $|\xi(x)| < 10^{-9}$). In total, it takes 7315.9 s to generate $n = 10^6$ samples. The estimated mean value is -3.8×10^{-3} and the statistical error is 3.8×10^{-3}.

The empirical density distributions of $\mathrm{Tr}(x)$ using both the scheme (3.8) and the algorithm in [43] are shown in the left plot of Figure 5, while the autocorrelation functions are plotted in the right plot of Figure 5. From these results, we can conclude that in this example both approaches provide similar statistical estimations (the autocorrelation time using Metropolis-adjusted method is slightly smaller with the above parameters). At the same time, the total computational time using the scheme (3.8) is less than half of the computational time required by the algorithm in [43]. For this example, although the average number of Newton steps in the latter algorithm is smaller than the average number of ODE iterations, the computational cost of each Newton step is indeed larger. We refer to Remark 3.9 for the comparison of computational complexity of both approaches.

Example 3: Removing stiffness by choosing a non-constant matrix a

In this example, we choose the reaction coordinate function

$$\xi(x) = \xi(x_1, x_2, \ldots, x_d) = \frac{1}{2}\left(x_1^2 + x_2^2 + \ldots + x_d^2 - 1\right).$$

Correspondingly, the level set

$$\Sigma = \left\{(x_1, x_2, \ldots, x_d) \in \mathbb{R}^d \;\middle|\; x_1^2 + x_2^2 + \ldots + x_d^2 = 1\right\}$$

is the $(d-1)$-dimensional unit sphere, and we have

$$\nabla\xi = (x_1, x_2, \ldots, x_d)^T, \quad \nabla\xi^T\nabla\xi = \sum_{i=1}^{d} x_i^2.$$

In the following, we give an example to show that in some applications it is helpful to use a non-constant matrix a in the numerical scheme (3.8). Briefly speaking, varying the matrix a properly allows to rescale the scheme along different directions. It has a preconditioning effect when different time scales (stiffness) exist.

[2]The roles of the proposal length scale in [43] and the step-size h in the scheme (3.8) are different. The proposal length scale 0.257 used in this example corresponds to a step-size 0.033 ($\approx 0.257^2/2$) in the scheme (3.8).

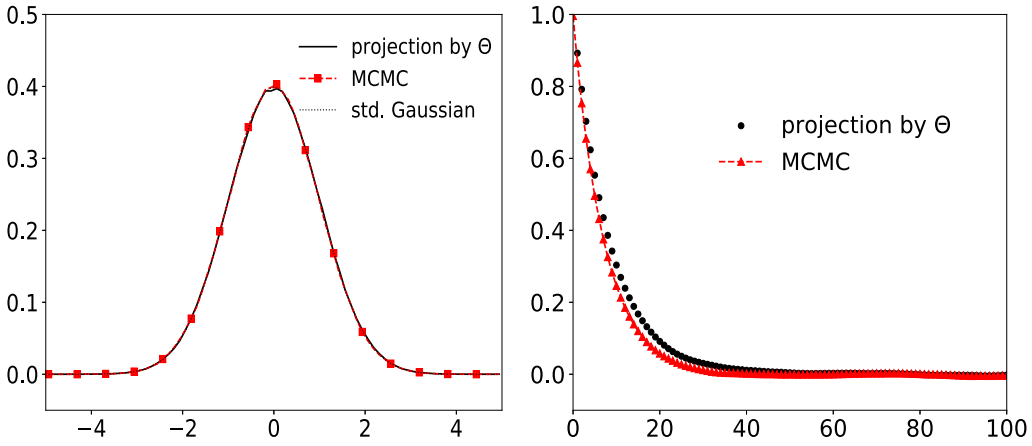

FIGURE 5. Example 2. Left: empirical density plots of the statistics $\mathrm{Tr}(x)$, where $x \in \mathrm{SO}(11)$. Both empirical densities resemble the probability density of the standard Gaussian random variable. Right: autocorrelation functions of the sampled trajectories. In both plots, the curve with label "projection by Θ" and the curve with label "MCMC" are the results obtained using the scheme (3.8) and the Metropolis-adjusted algorithm in [43], respectively.

Consider $d = 3$ and the potential $U = \frac{\theta^2}{2\epsilon}$, where $\epsilon > 0$ is a small parameter, θ is the angle of the state $x = (x_1, x_2, x_3)$ under the spherical coordinate system

$$x_1 = \rho\cos\theta\cos\varphi, \quad x_2 = \rho\cos\theta\sin\varphi, \quad x_3 = \rho\sin\theta,$$

where $\rho \geq 0$, $\theta \in [-\frac{\pi}{2}, \frac{\pi}{2}]$, and $\varphi \in [0, 2\pi]$. We can verify that

$$\nabla\theta = \frac{1}{\rho^2}\left(-\frac{x_1x_3}{(x_1^2+x_2^2)^{\frac{1}{2}}}, -\frac{x_2x_3}{(x_1^2+x_2^2)^{\frac{1}{2}}}, (x_1^2+x_2^2)^{\frac{1}{2}}\right)^T. \tag{4.11}$$

Correspondingly, with the choice of $\sigma = a = \mathrm{id}$, the scheme (3.8) is

$$\begin{aligned} x^{(l+\frac{1}{2})} &= x^{(l)} - \frac{1}{\epsilon}(\theta\nabla\theta)(x^{(l)})\,h + \sqrt{2\beta^{-1}h}\,\boldsymbol{\eta}^{(l)}, \\ x^{(l+1)} &= \Theta\big(x^{(l+\frac{1}{2})}\big), \end{aligned} \tag{4.12}$$

where $\nabla\theta$ is given in (4.11). Notice that, the coefficients in (4.12) are $\mathcal{O}(\frac{1}{\epsilon})$ when ϵ is small. In particular, it implies that sampling the invariant measure using (4.12) will be inefficient when ϵ is small, since the step-size h will be severely limited due to the large magnitude of the coefficients in (4.12).

On the other hand, based on the form of U and the expression (4.11), we consider the orthogonal vectors

$$\begin{aligned} \boldsymbol{\sigma}_1 &= (x_1, x_2, x_3)^T = \nabla\xi, \quad \boldsymbol{\sigma}_2 = (x_2, -x_1, 0)^T, \\ \boldsymbol{\sigma}_3 &= \left(-\frac{\sqrt{\epsilon}\,x_1x_3}{(x_1^2+x_2^2)^{\frac{1}{2}}}, -\frac{\sqrt{\epsilon}\,x_2x_3}{(x_1^2+x_2^2)^{\frac{1}{2}}}, \sqrt{\epsilon}(x_1^2+x_2^2)^{\frac{1}{2}}\right)^T = \sqrt{\epsilon}\rho^2\nabla\theta, \end{aligned}$$

and we define $\sigma = (\boldsymbol{\sigma}_1, \boldsymbol{\sigma}_2, \boldsymbol{\sigma}_3) \in \mathbb{R}^{3\times 3}$. Direct calculation shows that

$$a = \sigma\sigma^T = \begin{pmatrix} x_1^2 + x_2^2 + \frac{\epsilon x_1^2x_3^2}{x_1^2+x_2^2} & \frac{\epsilon x_1x_2x_3^2}{x_1^2+x_2^2} & (1-\epsilon)x_1x_3 \\ \frac{\epsilon x_1x_2x_3^2}{x_1^2+x_2^2} & x_1^2 + x_2^2 + \frac{\epsilon x_2^2x_3^2}{x_1^2+x_2^2} & (1-\epsilon)x_2x_3 \\ (1-\epsilon)x_1x_3 & (1-\epsilon)x_2x_3 & x_3^2 + \epsilon(x_1^2+x_2^2) \end{pmatrix}. \tag{4.13}$$

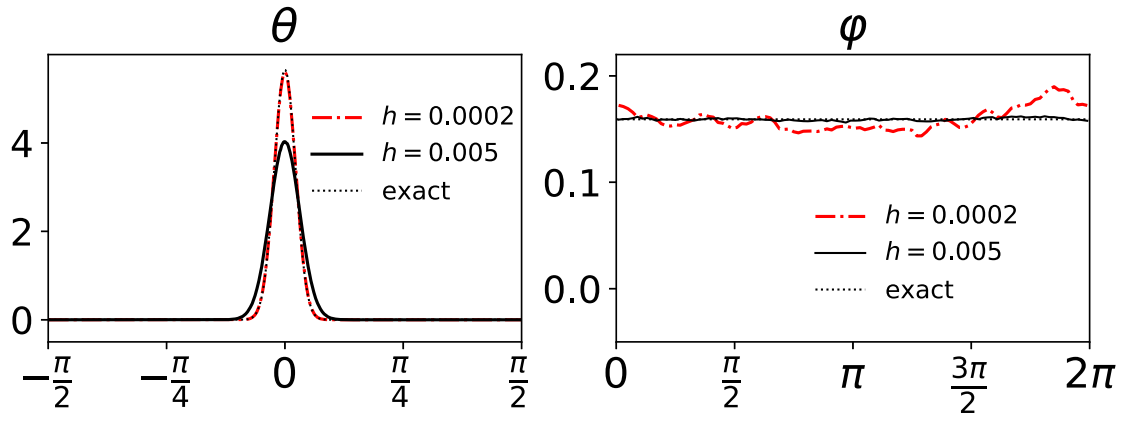

FIGURE 6. Example 3. The empirical densities of the angles θ and φ are estimated using the scheme (4.12) which corresponds to $a = \mathrm{id}$. $\epsilon = 0.005$ and $n = 10^7$ states are sampled, using a small step-size $h = 0.0002$ and a larger step-size $h = 0.005$. The curves with label "exact" are the analytical marginal densities computed from (4.16).

Correspondingly, using (4.13), the scheme (3.8) becomes

$$\begin{aligned} x_i^{(l+\frac{1}{2})} &= x_i^{(l)} + \left[-\theta \frac{\partial \theta}{\partial x_i} + \frac{1}{\beta}\frac{\partial a_{ij}}{\partial x_j}\right](x^{(l)})\, h + \sqrt{2\beta^{-1}h}\,\sigma_{ij}(x^{(l)})\,\boldsymbol{\eta}_j^{(l)}, \quad 1 \le i \le 3, \\ x^{(l+1)} &= \Theta\big(x^{(l+\frac{1}{2})}\big), \end{aligned} \tag{4.14}$$

where $\Theta(x)$ is the limit of the ODE flow

$$\dot{y}(s) = -\xi\big(y(s)\big)\left(2\xi\big(y(s)\big) + 1\right) y(s), \quad y(0) = x. \tag{4.15}$$

Importantly, in contrast to (4.12), the scheme (4.14) and (4.15) is no longer stiff when ϵ is small.

Now we compare the numerical efficiency between the schemes (4.12), (4.14) and (4.15). First of all, since the surface measure on Σ satisfies $\mathrm{d}\nu = \cos\theta \mathrm{d}\theta\, \mathrm{d}\varphi$, we know that the target measure is

$$\mathrm{d}\mu = \frac{1}{Z}\mathrm{e}^{-\frac{\beta\theta^2}{2\epsilon}}\,\mathrm{d}\nu = \frac{1}{Z}\mathrm{e}^{-\frac{\beta\theta^2}{2\epsilon}}\cos\theta\,\mathrm{d}\theta\,\mathrm{d}\varphi. \tag{4.16}$$

In the numerical study, we choose $\epsilon = 0.005$ and generate $n = 10^7$ states for both schemes. For the scheme (4.12) which corresponds to $a = \mathrm{id}$, we use both a small step-size $h = 0.0002$ and a (relatively) larger step-size $h = 0.005$, while we choose a large step-size $h = 0.01$ in the scheme (4.14) and (4.15). The empirical probability densities of the angles θ, φ for the two schemes are shown in Figures 6 and 7, respectively. From Figure 6, we see that the step-size h has to be small ($h = 0.0002$) in (4.12) in order to produce the correct probability density of the angle θ (left plot). However, with such a small h, the estimated empirical density of the angle φ (right plot) is still noisy with $n = 10^7$. On the other hand, for the scheme (4.14) and (4.15) which corresponds to the matrix a in (4.13), Figure 7 shows that the probability densities of both angles θ, φ are well approximated using the large step-size $h = 0.01$. Therefore, we conclude that in this example choosing the non-constant matrix a in (4.13) indeed helps improve the sampling efficiency.

5. Conclusions

Ergodic diffusion processes on a submanifold of $\mathbb{R}^d$ and related numerical sampling schemes have been considered in this work. A family of SDEs has been obtained whose invariant measures coincide with the given

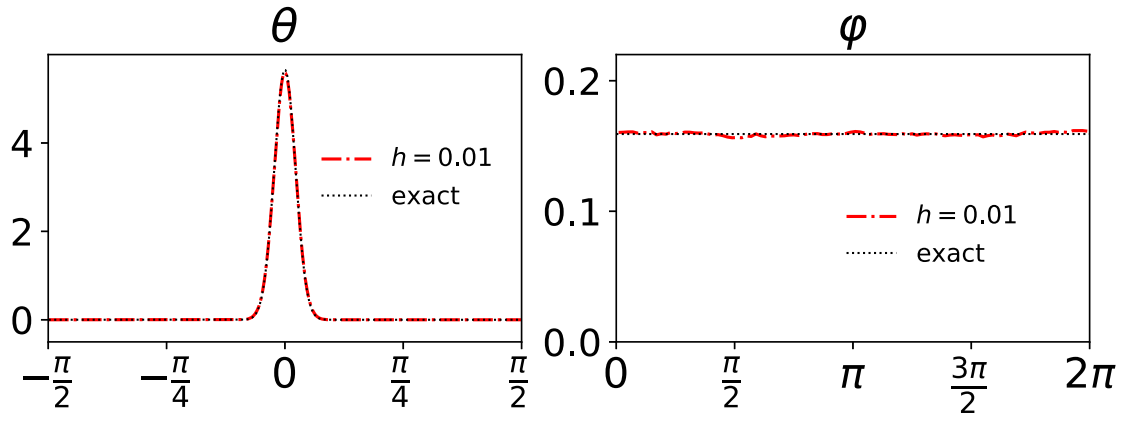

FIGURE 7. Example 3. The empirical densities of the angles θ and φ are estimated using the scheme (4.14) and (4.15) which corresponds to the matrix a in (4.13). $\epsilon = 0.005$ and $n = 10^7$ states are sampled using a large step-size $h = 0.01$. The curves with label "exact" are the analytical marginal densities computed from (4.16).

probability measure on the submanifold. In particular, for the conditional probability measure, we found that the corresponding SDEs have a relatively simple form. We proposed and analyzed a consistent numerical scheme which only requires 1st order derivatives of the reaction coordinate function. Different sampling schemes on the submanifolds are numerically evaluated.

The current work extends results in the literature and may further contribute to both the analysis and the development of numerical methods on related problems, in particular problems in molecular dynamics such as free energy calculation and model reduction of high-dimensional stochastic processes. Closely related to the current paper, the following topics could be considered. First, the "non-reversible" scheme (3.17) is supported by a simple numerical example but theoretical justification still needs to be investigated. This will be considered in future following the approach described in Remark 3.8. Second, the constrained numerical schemes in the current work do not involve system's momentum variables. In view of the work [31], it is interesting to study the Langevin dynamics under different constraints (such as certain variants of the map Θ used in this work). Third, there is a research interest in the literature to study the effective dynamics of molecular systems along a given reaction coordinate ξ. The coefficients of the effective dynamics are usually defined as averages on the level set of ξ [26]. As an application of the numerical scheme proposed in this work, we will study numerical algorithms to simulate the effective dynamics. This topic is related to the heterogeneous multiscale methods [42] and the equation-free approach [23, 25] in the literature.

APPENDIX A. USEFUL FACTS ABOUT THE RIEMANNIAN MANIFOLD $\mathcal{M}$

In this section, we present technical details of Section 2 related to the Riemannian manifold $\mathcal{M} = (\mathbb{R}^d, g)$, where $g = a^{-1}$. The main result is Proposition A.3, where we give the expression of the Laplacian–Beltrami operator Δ^Σ on the level set Σ in (1.1), viewed as a submanifold of $\mathcal{M}$. Before that, we first introduce some notations and quantities related to $\mathcal{M}$ and Σ. Readers are referred to [6, 12, 21, 37] for related discussions on general Riemannian manifolds.

Under Assumption 1.1, given two vectors $\boldsymbol{u} = (u_1, u_2, \ldots, u_d)^T$, $\boldsymbol{v} = (v_1, v_2, \ldots, v_d)^T$, we consider the space $\mathbb{R}^d$ with the weighted inner product

$$g(\boldsymbol{u}, \boldsymbol{v}) = \langle \boldsymbol{u}, \boldsymbol{v} \rangle_g = u_i (a^{-1})_{ij} v_j. \tag{A.1}$$

The inner product in (A.1) defines a Riemannian metric g on $\mathbb{R}^d$ and we denote by $\mathcal{M} = (\mathbb{R}^d, g)$ the Riemannian manifold $\mathbb{R}^d$ endowed with this metric.

Notice that $\mathcal{M}$ as a manifold is quite special (simple), in that it has a natural global coordinate chart which is given by the usual Euclidean coordinate. Since we will always work with this coordinate, we will not distinguish between tangent vectors (operators acting on functions) and their coordinate representations (d-dimensional vectors). In particular, $\boldsymbol{e}_i$ denotes the vector whose ith component equals to 1 while all the other $d-1$ components equal to 0, where $1 \le i \le d$. At each point $x \in \mathcal{M}$, vectors $\boldsymbol{e}_1, \boldsymbol{e}_2, \ldots, \boldsymbol{e}_d$ form a basis of the tangent space $T_x\mathcal{M}$ and under this basis we have $g = a^{-1}$, as can be seen from (A.1).

Denote by $\mathrm{grad}^{\mathcal{M}}$, $\mathrm{div}^{\mathcal{M}}$ the gradient and the divergence operator on $\mathcal{M}$, respectively. For any smooth function $f : \mathcal{M} \to \mathbb{R}$, it is direct to verify that

$$\mathrm{grad}^{\mathcal{M}} f = g^{ij} \frac{\partial f}{\partial x_j} \boldsymbol{e}_i = (a\nabla f)_i \, \boldsymbol{e}_i \,,$$

where $g^{ij} = (g^{-1})_{ij} = a_{ij}$, and ∇f denotes the ordinary gradient operator for functions on the Euclidean space $\mathbb{R}^d$. For simplicity, we will also write $\partial_i f$ for the partial derivative with respect to x_i, and $(a\nabla f)_i$ to denote the ith component of the vector $a\nabla f$, *i.e.*, $\partial_i f = \frac{\partial f}{\partial x_i}$, and $(a\nabla f)_i = a_{ij} \frac{\partial f}{\partial x_j} = a_{ij}\partial_j f$.

The Laplace–Beltrami operator on $\mathcal{M}$ is defined by $\Delta^{\mathcal{M}} f = \mathrm{div}^{\mathcal{M}}(\mathrm{grad}^{\mathcal{M}} f)$. Equivalently, we have $\Delta^{\mathcal{M}} f = \mathrm{tr}(\mathrm{Hess}^{\mathcal{M}} f)$, where $\mathrm{Hess}^{\mathcal{M}}$ is the Hessian operator on $\mathcal{M}$. The integration by parts formula on $\mathcal{M}$ has the form

$$\int_{\mathcal{M}} (\Delta^{\mathcal{M}} f_1)\, f_2 \, \mathrm{d}m = -\int_{\mathcal{M}} \langle \mathrm{grad}^{\mathcal{M}} f_1, \mathrm{grad}^{\mathcal{M}} f_2 \rangle_g \, \mathrm{d}m = \int_{\mathcal{M}} (\Delta^{\mathcal{M}} f_2) f_1 \, \mathrm{d}m, \tag{A.2}$$

for $\forall f_1,\, f_2 \in C_0^\infty(\mathcal{M})$, where $\mathrm{d}m = (\det g)^{\frac{1}{2}} \, \mathrm{d}x = (\det a)^{-\frac{1}{2}} \, \mathrm{d}x$ is the volume form, and $C_0^\infty(\mathcal{M})$ consists of all smooth functions on $\mathcal{M}$ with compact support.

Besides the vector basis $\boldsymbol{e}_1, \boldsymbol{e}_2, \ldots, \boldsymbol{e}_d$, the vectors

$$\boldsymbol{\sigma}_i = (\sigma_{1i}, \sigma_{2i}, \ldots, \sigma_{di})^T, \quad 1 \le i \le d, \tag{A.3}$$

will also be useful. Note that $a = \sigma\sigma^T = g^{-1}$ implies $\langle \boldsymbol{\sigma}_i, \boldsymbol{\sigma}_j \rangle_g = (a^{-1})_{rl}\sigma_{ri}\sigma_{lj} = \delta_{ij}$. In other words, $\boldsymbol{\sigma}_1, \boldsymbol{\sigma}_2, \ldots, \boldsymbol{\sigma}_d$ form an orthonormal basis of $T_x\mathcal{M}$ at each $x \in \mathcal{M}$.

Denote by $\nabla^{\mathcal{M}}$ the Levi-Civita connection on $\mathcal{M}$. Given $x \in \mathcal{M}$ and a tangent vector $\boldsymbol{v} \in T_x\mathcal{M}$, $\nabla^{\mathcal{M}}_{\boldsymbol{v}}$ is the covariant derivative operator on $\mathcal{M}$ along the vector $\boldsymbol{v}$. For two vectors $\boldsymbol{u} = (u_1, u_2, \ldots, u_d)^T$, $\boldsymbol{v} = (v_1, v_2, \ldots, v_d)^T$, the Hessian of a smooth function $f : \mathcal{M} \to \mathbb{R}$ is defined as

$$\mathrm{Hess}^{\mathcal{M}} f(\boldsymbol{u}, \boldsymbol{v}) = \boldsymbol{u}(\boldsymbol{v} f) - (\nabla^{\mathcal{M}}_{\boldsymbol{u}} \boldsymbol{v}) f = u_i v_j \mathrm{Hess}^{\mathcal{M}} f(\boldsymbol{e}_i, \boldsymbol{e}_j) = u_i v_j \left(\frac{\partial^2 f}{\partial x_i \partial x_j} - \Gamma^l_{ij} \frac{\partial f}{\partial x_l} \right), \tag{A.4}$$

where

$$\Gamma^l_{ij} = \frac{1}{2} g^{lr} \left(\frac{\partial g_{ir}}{\partial x_j} + \frac{\partial g_{jr}}{\partial x_i} - \frac{\partial g_{ij}}{\partial x_r} \right) = \frac{1}{2} a_{lr} \left(\frac{\partial (a^{-1})_{ir}}{\partial x_j} + \frac{\partial (a^{-1})_{jr}}{\partial x_i} - \frac{\partial (a^{-1})_{ij}}{\partial x_r} \right), \quad 1 \le i, j, l \le d \tag{A.5}$$

are the Christoffel's symbols defined by $\nabla^{\mathcal{M}}_{\boldsymbol{e}_i} \boldsymbol{e}_j = \Gamma^l_{ij} \boldsymbol{e}_l$, for $1 \le i, j \le d$.

Now let us consider the level set

$$\Sigma = \xi^{-1}(\boldsymbol{0}) = \left\{ x \in \mathcal{M} = \mathbb{R}^d \;\middle|\; \xi(x) = \boldsymbol{0} \in \mathbb{R}^k \right\} \tag{A.6}$$

of the C^2 function $\xi : \mathbb{R}^d \to \mathbb{R}^k$ with $\xi = (\xi_1, \xi_2, \ldots, \xi_k)^T$, $1 \le k < d$. Applying regular value theorem [5], we know that Σ is a $(d-k)$-dimensional submanifold of $\mathcal{M}$, under Assumption 1.2.

Given $x \in \Sigma$ and a vector $\boldsymbol{v} \in T_x\mathcal{M}$, the orthogonal projection operator ($d \times d$ matrix) $P : \mathbb{R}^d \to T_x\Sigma$ is defined such that $\langle \boldsymbol{v} - P\boldsymbol{v}, \boldsymbol{u}\rangle_g = 0$, for $\forall\, \boldsymbol{u} \in T_x\Sigma$. It is straightforward to verify that $P = \mathrm{id} - a\nabla\xi\Psi^{-1}\nabla\xi^T$, or entry-wise,

$$P_{ij} = \delta_{ij} - (\Psi^{-1})_{\alpha\gamma}\,(a\,\nabla\xi_\alpha)_i\partial_j\xi_\gamma, \quad 1 \le i, j \le d, \tag{A.7}$$

where Ψ is the invertible $k \times k$ symmetric matrix at each point $x \in \Sigma$, given by

$$\Psi_{\alpha\gamma} = \langle \mathrm{grad}^{\mathcal{M}}\xi_\alpha, \mathrm{grad}^{\mathcal{M}}\xi_\gamma\rangle_g = (\nabla\xi^T a\nabla\xi)_{\alpha\gamma}, \quad 1 \le \alpha, \gamma \le k. \tag{A.8}$$

In the above, $\nabla\xi$ denotes the $d \times k$ matrix with entries $(\nabla\xi)_{i\alpha} = \partial_i\xi_\alpha$, for $1 \le \alpha \le k$, $1 \le i \le d$. We can verify that

$$aP^T = Pa, \quad P^2 = P, \quad P^T\nabla\xi_\alpha = 0, \quad 1 \le \alpha \le k. \tag{A.9}$$

Let us further assume that $\boldsymbol{v} \in T_x\Sigma$ is a tangent vector of Σ at x. Since $\{\boldsymbol{\sigma}_i\}_{1\le i\le d}$ forms an orthonormal basis of the tangent space $T_x\mathcal{M}$, we have $\boldsymbol{v} = \langle \boldsymbol{v}, \boldsymbol{\sigma}_i\rangle_g\boldsymbol{\sigma}_i$. Using the fact that $P\boldsymbol{v} = \boldsymbol{v}$, we obtain $\boldsymbol{v} = \langle \boldsymbol{v}, \boldsymbol{p}_i\rangle_g\boldsymbol{p}_i$, where $\boldsymbol{p}_i = P\boldsymbol{\sigma}_i \in T_x\Sigma$. If we denote $\boldsymbol{p}_i = P_{i,j}\boldsymbol{e}_j$, then it follows from (A.7) to (A.9) that

$$\begin{aligned} P_{i,j} &= (P\sigma)_{ji} = \sigma_{ji} - (\Psi^{-1})_{\alpha\gamma}(a\nabla\xi_\alpha)_j(\sigma^T\nabla\xi_\gamma)_i \\ P_{l,i}P_{l,j} &= (Pa)_{ij} = (aP^T)_{ij} = a_{ij} - (\Psi^{-1})_{\alpha\gamma}(a\nabla\xi_\alpha)_i(a\nabla\xi_\gamma)_j, \end{aligned} \tag{A.10}$$

for $1 \le i, j \le d$.

Let grad^Σ, div^Σ, Δ^Σ, Hess^Σ denote the gradient operator, the divergence operator, the Laplace–Beltrami operator and the Hessian operator on Σ, respectively. It is direct to check that the Levi-Civita connection and the gradient operator on Σ are given by $\nabla^\Sigma = P\nabla^{\mathcal{M}}$ and $\mathrm{grad}^\Sigma = P\,\mathrm{grad}^{\mathcal{M}}$, respectively. In particular, for $f \in C^\infty(\Sigma)$ and let $\widetilde{f}$ be its extension to $\mathcal{M}$ such that $\widetilde{f} \in C^\infty(\mathcal{M})$ and $\widetilde{f}|_\Sigma = f$, we have

$$\mathrm{grad}^\Sigma f = P\mathrm{grad}^{\mathcal{M}}\widetilde{f} = Pa\nabla\widetilde{f}.$$

Let ν_g be the surface measure on Σ induced from the metric g on $\mathcal{M}$. We recall that the mean curvature vector H on Σ is defined such that [2, 10]

$$\int_\Sigma \mathrm{div}^\Sigma\boldsymbol{v}\,\mathrm{d}\nu_g = -\int_\Sigma \langle H, \boldsymbol{v}\rangle_g\,\mathrm{d}\nu_g, \tag{A.11}$$

for all vector fields $\boldsymbol{v}$ on $\mathcal{M}$.

We have the following lemma, concerning the operators on Σ.

Lemma A.1. *Let $f \in C^\infty(\Sigma)$ and $\widetilde{f} \in C^\infty(\mathcal{M})$ be its extension to $\mathcal{M}$. $\boldsymbol{u} \in \Gamma(T\mathcal{M})$ is a tangent vector field on $\mathcal{M}$ and we recall the vectors $\boldsymbol{p}_i = P\boldsymbol{\sigma}_i$, $1 \le i \le d$. We have*

(1) $\mathrm{div}^\Sigma\boldsymbol{u} = \langle \nabla^{\mathcal{M}}_{\boldsymbol{p}_i}\boldsymbol{u}, \boldsymbol{p}_i\rangle_g$.
(2) $(\mathrm{div}^\Sigma\boldsymbol{p}_i)\boldsymbol{p}_i + P\nabla^{\mathcal{M}}_{\boldsymbol{p}_i}\boldsymbol{p}_i = 0$.
(3) $\Delta^\Sigma f = \sum_{i=1}^d \boldsymbol{p}_i^2\widetilde{f} + (\mathrm{div}^\Sigma\boldsymbol{p}_i)\boldsymbol{p}_i\widetilde{f} = \sum_{i=1}^d \boldsymbol{p}_i^2\widetilde{f} - \big(P\nabla^{\mathcal{M}}_{\boldsymbol{p}_i}\boldsymbol{p}_i\big)\widetilde{f}$.
(4) $\Delta^\Sigma f = \mathrm{Hess}^{\mathcal{M}}\widetilde{f}(\boldsymbol{p}_i, \boldsymbol{p}_i) + H\widetilde{f}$, *where H is the mean curvature vector of the submanifold Σ.*
(5) *In the special case when $g = a = id$, we have $(div^\Sigma\boldsymbol{p}_i)\boldsymbol{p}_i = P\nabla^{\mathcal{M}}_{\boldsymbol{p}_i}\boldsymbol{p}_i = 0$, and $\Delta^\Sigma = \sum_{i=1}^d \boldsymbol{p}_i^2$.*

Proof. The first two assertions can be directly verified. Let us prove the last three assertions. Let $x \in \Sigma$ and assume that $\boldsymbol{v}_i$, $1 \le i \le d-k$, is an orthonormal basis of $T_x\Sigma$. We have $\boldsymbol{v}_i = \langle \boldsymbol{v}_i, \boldsymbol{p}_j\rangle_g\boldsymbol{p}_j$. For the third assertion, by definition,

$$\begin{aligned} \Delta^\Sigma f &= \mathrm{div}^\Sigma(\mathrm{grad}^\Sigma f) = \mathrm{div}^\Sigma\big(P\,\mathrm{grad}^{\mathcal{M}}\widetilde{f}\big) = \mathrm{div}^\Sigma\big(\langle \mathrm{grad}^{\mathcal{M}}\widetilde{f}, \boldsymbol{p}_i\rangle_g\,\boldsymbol{p}_i\big) \\ &= \mathrm{div}^\Sigma\big((\boldsymbol{p}_i\widetilde{f})\boldsymbol{p}_i\big) = \sum_{i=1}^d \boldsymbol{p}_i^2\widetilde{f} + (\mathrm{div}^\Sigma\boldsymbol{p}_i)\boldsymbol{p}_i\widetilde{f} = \sum_{i=1}^d \boldsymbol{p}_i^2\widetilde{f} - \big(P\nabla^{\mathcal{M}}_{\boldsymbol{p}_i}\boldsymbol{p}_i\big)\widetilde{f}, \end{aligned}$$

where the second assertion has been used in the last equality.

For the fourth assertion, starting from the third assertion, using the definition of $\mathrm{Hess}^{\mathcal{M}}$ in (A.4), and applying Proposition A.2 below, we obtain

$$\begin{aligned}\Delta^{\Sigma} f &= \sum_{i=1}^{d} \boldsymbol{p}_i^2 f - P\nabla^{\mathcal{M}}_{\boldsymbol{p}_i}\boldsymbol{p}_i f \\ &= \mathrm{Hess}^{\mathcal{M}} \widetilde{f}(\boldsymbol{p}_i,\boldsymbol{p}_i) + \left[(I-P)\nabla^{\mathcal{M}}_{\boldsymbol{p}_i}\boldsymbol{p}_i\right]\widetilde{f} = \mathrm{Hess}^{\mathcal{M}} \widetilde{f}(\boldsymbol{p}_i,\boldsymbol{p}_i) + H\widetilde{f}.\end{aligned}$$

For the last assertion, when $g = \mathrm{id}$, we have $\Gamma^l_{ij} \equiv 0$, for $\forall 1 \le i,j,l \le d$. Also, it follows from (A.10) that $P_{i,j} = P_{ij} = P_{ji}$ and $P_{il}P_{lj} = P_{ij}$. We obtain

$$\begin{aligned}(\mathrm{div}^{\Sigma}\boldsymbol{p}_i)\boldsymbol{p}_i &= \langle \nabla^{\mathcal{M}}_{\boldsymbol{p}_j}\boldsymbol{p}_i, \boldsymbol{p}_j\rangle_g\, \boldsymbol{p}_i \\ &= P_{j,l}P_{j,j'}P_{i,i'}\langle \nabla^{\mathcal{M}}_{\boldsymbol{e}_l}\big(P_{i,r}\boldsymbol{e}_r\big), \boldsymbol{e}_{j'}\rangle_g\, \boldsymbol{e}_{i'} \\ &= P_{lr}\frac{\partial P_{ir}}{\partial x_l}P_{ii'}\,\boldsymbol{e}_{i'} \\ &= \left[\frac{\partial P_{il}}{\partial x_l}P_{ii'} - \frac{\partial P_{lr}}{\partial x_l}P_{ri'}\right]\boldsymbol{e}_{i'} \\ &= 0,\end{aligned}$$

and the other assertions follow accordingly. □

Proposition A.2. *Let H be the mean curvature vector defined in (A.11) on the submanifold Σ. We have*

$$\begin{aligned}H &= (I-P)\nabla^{\mathcal{M}}_{\boldsymbol{p}_i}\boldsymbol{p}_i \\ &= -(\Psi^{-1})_{\alpha\gamma}\left[\frac{1}{2}(Pa)_{ij}(a\nabla\xi_\alpha)_l\frac{\partial(a^{-1})_{ij}}{\partial x_l} + P_{il}\frac{\partial(a\nabla\xi_\alpha)_l}{\partial x_i}\right]a\nabla\xi_\gamma.\end{aligned} \tag{A.12}$$

In the special case when $g = a = \mathrm{id}$, we have

$$H = P_{jl}\frac{\partial P_{il}}{\partial x_j}\boldsymbol{e}_i = -\left[(\Psi^{-1})_{\alpha\gamma}P_{ij}\,\partial^2_{ij}\xi_\alpha\right]\nabla\xi_\gamma. \tag{A.13}$$

Proof. Given a tangent vector field $\boldsymbol{v}$ on $\mathcal{M}$, from the definition of P we have $\boldsymbol{v} = P\boldsymbol{v} + (\Psi^{-1})_{\alpha\gamma}\langle \boldsymbol{v}, a\nabla\xi_\gamma\rangle_g\, a\nabla\xi_\alpha$. Since $P\boldsymbol{v}$ is a tangent vector field on Σ, using (A.11) and the divergence theorem on Σ, we know

$$\int_\Sigma \langle H,\boldsymbol{v}\rangle_g\,\mathrm{d}\nu_g = -\int_\Sigma \mathrm{div}^{\Sigma}\left[(I-P)\boldsymbol{v}\right]\mathrm{d}\nu_g = -\int_\Sigma \mathrm{div}^{\Sigma}\left[(\Psi^{-1})_{\alpha\gamma}\langle\boldsymbol{v}, a\nabla\xi_\gamma\rangle_g\, a\nabla\xi_\alpha\right]\mathrm{d}\nu_g. \tag{A.14}$$

For the first expression, we notice that $\langle (I-P)\boldsymbol{v}, \boldsymbol{p}_i\rangle_g \equiv 0$, $1 \le i \le d$. Applying Lemma A.1, we have

$$\begin{aligned}-\int_\Sigma \mathrm{div}^{\Sigma}\left[(I-P)\boldsymbol{v}\right]\mathrm{d}\nu_g &= -\int_\Sigma \langle \nabla^{\mathcal{M}}_{\boldsymbol{p}_i}\left[(I-P)\boldsymbol{v}\right], \boldsymbol{p}_i\rangle_g\,\mathrm{d}\nu_g \\ &= -\int_\Sigma \boldsymbol{p}_i\langle (I-P)\boldsymbol{v}, \boldsymbol{p}_i\rangle_g\,\mathrm{d}\nu_g + \int_\Sigma \langle (I-P)\boldsymbol{v}, \nabla^{\mathcal{M}}_{\boldsymbol{p}_i}\boldsymbol{p}_i\rangle_g\,\mathrm{d}\nu_g \\ &= \int_\Sigma \langle \boldsymbol{v}, (I-P)\nabla^{\mathcal{M}}_{\boldsymbol{p}_i}\boldsymbol{p}_i\rangle_g\,\mathrm{d}\nu_g.\end{aligned}$$

Comparing the last equality above with (A.14), we conclude that $H = (I-P)\nabla^{\mathcal{M}}_{\boldsymbol{p}_i}\boldsymbol{p}_i$.

For the second expression, we notice that $\langle a\nabla\xi_\alpha, \boldsymbol{p}_i\rangle_g = 0$, and also recall the expressions (A.5), (A.8) and (A.10). Applying Lemma A.1, integrating by parts, and noticing the cancellation of some terms, we can derive

$$\begin{aligned}
\operatorname{div}^\Sigma\left[(\Psi^{-1})_{\alpha\gamma}\langle \boldsymbol{v}, a\nabla\xi_\gamma\rangle_g\, a\nabla\xi_\alpha\right] &= \langle \nabla^{\mathcal{M}}_{\boldsymbol{p}_i}\left[(\Psi^{-1})_{\alpha\gamma}\langle \boldsymbol{v}, a\nabla\xi_\gamma\rangle_g\, a\nabla\xi_\alpha\right], \boldsymbol{p}_i\rangle_g \\
&= (\Psi^{-1})_{\alpha\gamma}\langle \boldsymbol{v}, a\nabla\xi_\gamma\rangle_g\, \langle \nabla^{\mathcal{M}}_{\boldsymbol{p}_i}(a\nabla\xi_\alpha), \boldsymbol{p}_i\rangle_g \\
&= (\Psi^{-1})_{\alpha\gamma}\langle \boldsymbol{v}, a\nabla\xi_\gamma\rangle_g\, P_{i,j}P_{i,l}\langle \nabla^{\mathcal{M}}_{\boldsymbol{e}_j}\big((a\nabla\xi_\alpha)_r\boldsymbol{e}_r\big), \boldsymbol{e}_l\rangle_g \\
&= (\Psi^{-1})_{\alpha\gamma}\langle \boldsymbol{v}, a\nabla\xi_\gamma\rangle_g\, (Pa)_{jl}\left[(a\nabla\xi_\alpha)_r\Gamma^i_{jr}(a^{-1})_{il} + \frac{\partial(a\nabla\xi_\alpha)_r}{\partial x_j}(a^{-1})_{lr}\right] \\
&= (\Psi^{-1})_{\alpha\gamma}\langle \boldsymbol{v}, a\nabla\xi_\gamma\rangle_g\, (Pa)_{ij}\left[\frac{1}{2}(a\nabla\xi_\alpha)_l\frac{\partial(a^{-1})_{ij}}{\partial x_l} + \frac{\partial(a\nabla\xi_\alpha)_l}{\partial x_i}(a^{-1})_{lj}\right].
\end{aligned}$$

The second identity in (A.12) is obtained after comparing the above expression with (A.14).

In the case $g = a = \mathrm{id}$, we have $\Gamma^r_{il} \equiv 0$, $1 \le i, l, r \le d$. It follows that

$$\operatorname{div}^\Sigma\left[(\Psi^{-1})_{\alpha\gamma}\langle \boldsymbol{v}, a\nabla\xi_\gamma\rangle_g\, a\nabla\xi_\alpha\right] = (\Psi^{-1})_{\alpha\gamma}\langle \boldsymbol{v}, a\nabla\xi_\gamma\rangle_g\, P_{ij}\,\partial^2_{ij}\xi_\alpha$$

and we obtain that $H = -\left[(\Psi^{-1})_{\alpha\gamma}P_{ij}\,\partial^2_{ij}\xi_\alpha\right]\nabla\xi_\gamma$. Using (A.7) and (A.9), we have

$$P_{jl}\frac{\partial P_{il}}{\partial x_j}\boldsymbol{e}_i = -P_{jl}\frac{\partial\big((\Psi^{-1})_{\alpha\gamma}\partial_l\xi_\alpha\partial_i\xi_\gamma\big)}{\partial x_j}\boldsymbol{e}_i = -\left[(\Psi^{-1})_{\alpha\gamma}P_{jl}\,\partial^2_{jl}\xi_\alpha\,\partial_i\xi_\gamma\right]\boldsymbol{e}_i = H,$$

and therefore the first expression in (A.13) holds as well. □

Next, we study the Laplace–Beltrami operator Δ^Σ on the submanifold Σ. Clearly, Δ^Σ is self-adjoint and, similar to (A.2), we have the integration by parts formula on Σ with respect to the measure ν_g, as

$$\int_\Sigma (\Delta^\Sigma f_1)\, f_2\, \mathrm{d}\nu_g = -\int_\Sigma \langle \operatorname{grad}^\Sigma f_1, \operatorname{grad}^\Sigma f_2\rangle_g\, \mathrm{d}\nu_g = \int_\Sigma (\Delta^\Sigma f_2) f_1\, \mathrm{d}\nu_g, \tag{A.15}$$

for $\forall f_1,\ f_2 \in C^\infty(\Sigma)$. The expression of Δ^Σ can be computed explicitly and this is the content of the following proposition.

Proposition A.3. *Let Σ be the submanifold of $\mathcal{M}$ defined in (A.6), P be the projection matrix in (A.7), and Δ^Σ be the Laplace–Beltrami operator on Σ. We have*

$$\Delta^\Sigma = (Pa)_{ij}\frac{\partial^2}{\partial x_i\partial x_j} + \left[\frac{\partial(Pa)_{ij}}{\partial x_j} + \frac{1}{2}(Pa)_{ij}\frac{\partial \ln\left((\det a)^{-1}\det(\nabla\xi^T a\nabla\xi)\right)}{\partial x_j}\right]\frac{\partial}{\partial x_i}. \tag{A.16}$$

In the special case when $g = a = \mathrm{id}$, we have

$$\begin{aligned}
\Delta^\Sigma &= \sum_{i=1}^d \boldsymbol{p}_i^2 = P_{ij}\frac{\partial^2}{\partial x_i\partial x_j} + P_{lj}\frac{\partial P_{li}}{\partial x_j}\frac{\partial}{\partial x_i} \\
&= P_{ij}\frac{\partial^2}{\partial x_i\partial x_j} + H_i\frac{\partial}{\partial x_i},
\end{aligned} \tag{A.17}$$

where $H = H_i\boldsymbol{e}_i$ is the mean curvature vector of the submanifold Σ.

Proof. Let $f \in C^\infty(\Sigma)$ and $\widetilde{f} \in C^\infty(\mathcal{M})$ be its extension to $\mathcal{M}$. Using Lemma A.1 and Proposition A.2, we have

$$\begin{aligned}\Delta^\Sigma f &= \mathrm{Hess}^{\mathcal{M}}\widetilde{f}(\boldsymbol{p}_r, \boldsymbol{p}_r) + H\widetilde{f} \\ &= P_{r,j}P_{r,l}\mathrm{Hess}^{\mathcal{M}}\widetilde{f}(\boldsymbol{e}_j, \boldsymbol{e}_l) + H\widetilde{f} \\ &= (Pa)_{jl}\left(\frac{\partial^2\widetilde{f}}{\partial x_j \partial x_l} - \Gamma^i_{jl}\frac{\partial\widetilde{f}}{\partial x_i}\right) \\ &\quad - (\Psi^{-1})_{\alpha\gamma}\left[\frac{1}{2}(Pa)_{jl}(a\nabla\xi_\gamma)_r\frac{\partial(a^{-1})_{jl}}{\partial x_r} + P_{lr}\frac{\partial(a\nabla\xi_\gamma)_r}{\partial x_l}\right](a\nabla\xi_\alpha)_i\frac{\partial\widetilde{f}}{\partial x_i}.\end{aligned}$$

Notice that we have already obtained the coefficients of the second order derivative terms. For the terms of the first order derivatives, let us denote

$$\begin{aligned}I_1 &= -(Pa)_{jl}\Gamma^i_{jl} \\ I_2 &= -\frac{1}{2}(\Psi^{-1})_{\alpha\gamma}(Pa)_{jl}(a\nabla\xi_\alpha)_i(a\nabla\xi_\gamma)_r\frac{\partial(a^{-1})_{jl}}{\partial x_r} \\ I_3 &= -(\Psi^{-1})_{\alpha\gamma}P_{lr}(a\nabla\xi_\alpha)_i\frac{\partial(a\nabla\xi_\gamma)_r}{\partial x_l}.\end{aligned} \tag{A.18}$$

Using the expression of Pa in (A.10), the property $Pa\nabla\xi_\gamma = 0$, and integrating by parts, we easily obtain

$$\begin{aligned}I_2 &= \frac{1}{2}\big((Pa)_{ir} - a_{ir}\big)(Pa)_{jl}\frac{\partial(a^{-1})_{jl}}{\partial x_r} \\ I_3 &= \frac{\partial P_{lr}}{\partial x_l}\big(a_{ir} - (Pa)_{ir}\big).\end{aligned} \tag{A.19}$$

For I_1, direct calculation using (A.5) gives

$$\begin{aligned}I_1 &= -\frac{1}{2}(Pa)_{jl}a_{ir}\left(\frac{\partial(a^{-1})_{lr}}{\partial x_j} + \frac{\partial(a^{-1})_{jr}}{\partial x_l} - \frac{\partial(a^{-1})_{jl}}{\partial x_r}\right) \\ &= -(Pa)_{jl}a_{ir}\frac{\partial(a^{-1})_{lr}}{\partial x_j} + \frac{1}{2}(Pa)_{jl}a_{ir}\frac{\partial(a^{-1})_{jl}}{\partial x_r} \\ &= \frac{\partial(Pa)_{ij}}{\partial x_j} - \frac{\partial P_{jr}}{\partial x_j}a_{ir} + \frac{1}{2}(Pa)_{jl}a_{ir}\frac{\partial(a^{-1})_{jl}}{\partial x_r}.\end{aligned} \tag{A.20}$$

Therefore,

$$\begin{aligned}I_1 + I_2 + I_3 &= \frac{\partial(Pa)_{ij}}{\partial x_j} - \frac{\partial P_{lr}}{\partial x_l}(Pa)_{ir} + \frac{1}{2}(Pa)_{jl}a_{ir}\frac{\partial(a^{-1})_{jl}}{\partial x_r} + \frac{1}{2}\big((Pa)_{ir} - a_{ir}\big)(Pa)_{jl}\frac{\partial(a^{-1})_{jl}}{\partial x_r} \\ &= \frac{\partial(Pa)_{ij}}{\partial x_j} - \frac{\partial P_{lr}}{\partial x_l}(Pa)_{ir} + \frac{1}{2}(Pa)_{ir}(Pa)_{jl}\frac{\partial(a^{-1})_{jl}}{\partial x_r}.\end{aligned}$$

Applying Lemma A.4 below to handle the last term above, we conclude

$$I_1 + I_2 + I_3 = \frac{\partial(Pa)_{ij}}{\partial x_j} - \frac{1}{2}(Pa)_{ir}\frac{\partial \ln\det a}{\partial x_r} + \frac{1}{2}(Pa)_{ir}\frac{\partial \ln\det\Psi}{\partial x_r}.$$

Finally, when $g = a = \mathrm{id}$, applying Lemma A.1, we can obtain

$$\begin{aligned}\Delta^{\Sigma} f &= \mathrm{Hess}^{\mathcal{M}} \widetilde{f}(\boldsymbol{p}_i, \boldsymbol{p}_i) + H\widetilde{f} \\ &= P_{l,i}P_{l,j}\left(\frac{\partial^2 \widetilde{f}}{\partial x_i \partial x_j} - \Gamma_{ij}^{l}\frac{\partial \widetilde{f}}{\partial x_l}\right) + H\widetilde{f} \\ &= P_{ij}\frac{\partial^2 \widetilde{f}}{\partial x_i \partial x_j} + H_i \frac{\partial \widetilde{f}}{\partial x_i}.\end{aligned}$$

The other equality in (A.17) follows from Proposition A.2. □

We point out that the proof of Proposition A.3 is indeed valid for a general Riemannian manifold $\mathcal{M}$ and its level set Σ as well. In this case, (A.16) holds true on a local coordinate of the manifold $\mathcal{M}$.

The following identity has been used in the above proof, and will be useful in Appendix B as well.

Lemma A.4.

$$\frac{1}{2}(Pa)_{ir}(Pa)_{jl}\frac{\partial (a^{-1})_{jl}}{\partial x_r} = -\frac{1}{2}(Pa)_{ir}\frac{\partial \ln\det a}{\partial x_r} + (Pa)_{ir}\frac{\partial P_{lr}}{\partial x_l} + \frac{1}{2}(Pa)_{ir}\frac{\partial \ln\det \Psi}{\partial x_r}.$$

Proof. Using the expression of Pa in (A.10), the relations

$$Pa\nabla\xi_\gamma = 0, \quad \frac{\partial \ln\det a}{\partial x_r} = (a^{-1})_{jl}\frac{\partial a_{jl}}{\partial x_r}, \quad \frac{\partial \ln\det \Psi}{\partial x_r} = (\Psi^{-1})_{\alpha\gamma}\frac{\partial \Psi_{\alpha\gamma}}{\partial x_r},$$

and the integration by parts formula, we can compute

$$\begin{aligned}\frac{1}{2}(Pa)_{ir}(Pa)_{jl}\frac{\partial (a^{-1})_{jl}}{\partial x_r} &= \frac{1}{2}(Pa)_{ir}\left(a_{jl} - (\Psi^{-1})_{\alpha\gamma}(a\nabla\xi_\alpha)_j(a\nabla\xi_\gamma)_l\right)\frac{\partial (a^{-1})_{jl}}{\partial x_r} \\ &= -\frac{1}{2}(Pa)_{ir}\frac{\partial \ln\det a}{\partial x_r} - \frac{1}{2}(Pa)_{ir}(\Psi^{-1})_{\alpha\gamma}(a\nabla\xi_\alpha)_l\,\partial^2_{lr}\xi_\gamma \\ &\quad + \frac{1}{2}(Pa)_{ir}(\Psi^{-1})_{\alpha\gamma}\partial_l\xi_\alpha\frac{\partial (a\nabla\xi_\gamma)_l}{\partial x_r} \\ &= -\frac{1}{2}(Pa)_{ir}\frac{\partial \ln\det a}{\partial x_r} - (Pa)_{ir}(\Psi^{-1})_{\alpha\gamma}(a\nabla\xi_\alpha)_l\,\partial^2_{lr}\xi_\gamma + \frac{1}{2}(Pa)_{ir}\frac{\partial \ln\det \Psi}{\partial x_r} \\ &= -\frac{1}{2}(Pa)_{ir}\frac{\partial \ln\det a}{\partial x_r} + (Pa)_{ir}\frac{\partial P_{lr}}{\partial x_l} + \frac{1}{2}(Pa)_{ir}\frac{\partial \ln\det \Psi}{\partial x_r}.\end{aligned}$$

□

We conclude this section with the proof of Corollary 2.6 in Section 2.

Proof of Corollary 2.6. Notice that the infinitesimal generator of (2.13) can be written as

$$\mathcal{L}^{\boldsymbol{J}} = J_i\frac{\partial}{\partial x_i} + \mathcal{L},$$

where $\mathcal{L}$ is the infinitesimal generator of (2.5). Using the fact $\boldsymbol{J} \in T_x\Sigma$, the same argument of Proposition 2.1 implies that (2.13) evolves on Σ as well. Since μ_1 is invariant with respect to $\mathcal{L}$, to show the SDE (2.13) has the same invariant measure, it is enough to verify that

$$\mathrm{div}^{\Sigma}\left\{\boldsymbol{J}\exp\left[-\beta\left(U + \frac{1}{2\beta}\ln\frac{\det(\nabla\xi^T a\nabla\xi)}{\det a}\right)\right]\right\} = 0, \quad \forall\, x \in \Sigma, \tag{A.21}$$

where we have used the expression of μ_1 in (2.7). Applying the formula of div^Σ in Lemma A.1, we can compute the right hand side of (A.21), as

$$\begin{aligned}
&\mathrm{div}^\Sigma \left\{ \boldsymbol{J} \exp\left[-\beta \left(U + \frac{1}{2\beta} \ln \frac{\det(\nabla\xi^T a \nabla\xi)}{\det a} \right) \right] \right\} \\
&= \left\langle \nabla^{\mathcal{M}}_{\boldsymbol{p}_j} \left\{ \exp\left[-\beta \left(U + \frac{1}{2\beta} \ln \frac{\det(\nabla\xi^T a \nabla\xi)}{\det a} \right) \right] J_i \boldsymbol{e}_i \right\}, \boldsymbol{p}_j \right\rangle_g \\
&= P_{j,l} P_{j,r} \left\langle \nabla^{\mathcal{M}}_{\boldsymbol{e}_l} \left\{ \exp\left[-\beta \left(U + \frac{1}{2\beta} \ln \frac{\det(\nabla\xi^T a \nabla\xi)}{\det a} \right) \right] J_i \boldsymbol{e}_i \right\}, \boldsymbol{e}_r \right\rangle_g .
\end{aligned}$$

which implies that (A.21) is equivalent to

$$\begin{aligned}
0 &= (Pa)_{lr} \frac{\partial J_i}{\partial x_l} (a^{-1})_{ir} + (Pa)_{lr} J_i \Gamma^{r'}_{li} (a^{-1})_{r'r} - \beta (Pa)_{lr} J_i (a^{-1})_{ir} \frac{\partial U}{\partial x_l} \\
&\quad - \frac{1}{2} (Pa)_{lr} J_i (a^{-1})_{ir} \frac{\partial}{\partial x_l} \left[\ln \frac{\det(\nabla\xi^T a \nabla\xi)}{\det a} \right] \\
&= P_{li} \frac{\partial J_i}{\partial x_l} + P_{lr'} J_i \Gamma^{r'}_{li} - \beta P_{li} J_i \frac{\partial U}{\partial x_l} - \frac{1}{2} P_{li} J_i \frac{\partial}{\partial x_l} \left[\ln \frac{\det(\nabla\xi^T a \nabla\xi)}{\det a} \right],
\end{aligned}$$

where $\Gamma^{r'}_{li}$ are the Christoffel's symbols satisfying $\nabla^{\mathcal{M}}_{\boldsymbol{e}_l} \boldsymbol{e}_i = \Gamma^{r'}_{li} \boldsymbol{e}_{r'}$. Using the expression (A.5) of $\Gamma^{r'}_{li}$, the fact $J_i = P_{ij} J_j$, and Lemma A.4, we can further simplify the above equation and obtain

$$\begin{aligned}
&P_{lr'} J_i \Gamma^{r'}_{li} - \frac{1}{2} P_{li} J_i \frac{\partial}{\partial x_l} \left[\ln \frac{\det(\nabla\xi^T a \nabla\xi)}{\det a} \right] \\
&= \frac{1}{2} J_i (Pa)_{lr} \frac{\partial (a^{-1})_{lr}}{\partial x_i} - \frac{1}{2} P_{li} J_i \frac{\partial}{\partial x_l} \left[\ln \frac{\det(\nabla\xi^T a \nabla\xi)}{\det a} \right] \\
&= J_j \frac{\partial P_{ij}}{\partial x_i}.
\end{aligned}$$

Therefore, we see that (A.21) is equivalent to the condition (2.12). □

Appendix B. Proofs in Section 3

In this section, we collect proofs of the various results in Section 3.

First, we prove Proposition 3.4, which concerns the properties of the flow map Θ defined in (3.4)–(3.6). While the approach of the proof is similar to the one in [13], here we consider the specific function F in (3.5) and we will provide full details of the derivations.

Proof of Proposition 3.4. In this proof, we will always assume $x \in \Sigma$. For a function which only depends on the state and is evaluated at x, we will often omit its argument in order to keep the notations simple. Also notice that, repeated indices other than l and l' indicate that they are summed up, while for the indices l, l' we assume that they are fixed by default unless the summation operator is used explicitly.

Since $\nabla F = 0$ on Σ, from the equation (3.4) we know that $\varphi(x, s) \equiv x$, $\forall s \geq 0$. Let us Denote by $\nabla^2 F$ the Hessian matrix (on the standard Euclidean space) of the function F in (3.5), *i.e.*, $\nabla^2 F = (\partial^2_{ij} F)_{1 \leq i,j \leq d}$. Since $\xi(x) = \mathbf{0} \in \mathbb{R}^k$, direct calculation gives

$$(a \nabla^2 F)_{ij} = a_{ir} \frac{\partial^2 F}{\partial x_r \partial x_j} = (a \nabla\xi \nabla\xi^T)_{ij}, \qquad 1 \leq i, j \leq d. \tag{B.1}$$

Meanwhile, it is straightforward to verify that $a\nabla^2 F$ satisfies

$$\begin{aligned}
&\langle a\nabla^2 F\boldsymbol{u},\boldsymbol{v}\rangle_g = \langle \boldsymbol{u}, a\nabla^2 F\boldsymbol{v}\rangle_g, && \forall\ \boldsymbol{u},\boldsymbol{v}\in\mathbb{R}^d,\\
&\langle a\nabla^2 F\boldsymbol{u},\boldsymbol{u}\rangle_g = |\nabla\xi^T\boldsymbol{u}|^2 \geq 0, && \forall\ \boldsymbol{u}\in\mathbb{R}^d,\\
&(a\nabla^2 F)\boldsymbol{u} = a\nabla\xi\nabla\xi^T\boldsymbol{u} = 0, && \forall\ \boldsymbol{u}\in T_x\Sigma.
\end{aligned}$$

Therefore, we can assume that $a\nabla^2 F$ has real (non-negative) eigenvalues

$$\lambda_1 = \lambda_2 = \ldots = \lambda_{d-k} = 0 < \lambda_{d-k+1} \leq \ldots \leq \lambda_d, \tag{B.2}$$

and the corresponding eigenvectors, denoted by $\boldsymbol{v}_i = (v_{i1}, v_{i2}, \ldots, v_{id})^T$, $1 \leq i \leq d$, are orthonormal with respect to the inner product $\langle\cdot,\cdot\rangle_g$ in (A.1), such that $\boldsymbol{v}_1, \boldsymbol{v}_2, \ldots, \boldsymbol{v}_{d-k} \in T_x\Sigma$.

The projection matrix P in (A.7) can be expressed using the vectors $\boldsymbol{v}_i$ as

$$P_{ij} = \sum_{l=1}^{d-k} v_{li}(a^{-1})_{jr}v_{lr}, \quad 1 \leq i,j \leq d, \tag{B.3}$$

and we have

$$\sum_{l=1}^{d-k} v_{li}v_{lj} = (Pa)_{ij}, \quad a_{ij} - (Pa)_{ij} = \sum_{l=d-k+1}^{d} v_{li}v_{lj}. \tag{B.4}$$

It is also a simple fact that the eigenvalues of the $k\times k$ matrix $\Psi = \nabla\xi^T a\nabla\xi$ are λ_{d-k+1}, λ_{d-k+2}, …, λ_d, with the corresponding eigenvectors given by $\nabla\xi^T\boldsymbol{v}_{d-k+1}$, $\nabla\xi^T\boldsymbol{v}_{d-k+2}$, …, $\nabla\xi^T\boldsymbol{v}_d$. In particular, this implies

$$\prod_{i=d-k+1}^{d} \lambda_i = \det(\nabla\xi^T a\nabla\xi) = \det\Psi. \tag{B.5}$$

In the following, we study the ODE (3.4) using the eigenvectors $\boldsymbol{v}_i$. Differentiating the ODE (3.4) twice, using the facts that $\varphi(x,s)\equiv x$, $\forall s\geq 0$, and $\nabla F = 0$ on Σ, we obtain

$$\begin{aligned}
\frac{\mathrm{d}}{\mathrm{d}s}\frac{\partial\varphi_i}{\partial x_j}(x,s) &= -\left(a_{ir'}\frac{\partial^2 F}{\partial x_{r'}\partial x_{i'}}\right)\frac{\partial\varphi_{i'}}{\partial x_j}(x,s)\\
\frac{\mathrm{d}}{\mathrm{d}s}\frac{\partial^2\varphi_i}{\partial x_j\partial x_r}(x,s) &= -\left(2\frac{\partial a_{ir'}}{\partial x_{i'}}\frac{\partial^2 F}{\partial x_{r'}\partial x_{j'}} + a_{ir'}\frac{\partial^3 F}{\partial x_{r'}\partial x_{i'}\partial x_{j'}}\right)\frac{\partial\varphi_{i'}}{\partial x_j}(x,s)\frac{\partial\varphi_{j'}}{\partial x_r}(x,s)\\
&\quad -\left(a_{ir'}\frac{\partial^2 F}{\partial x_{r'}\partial x_{i'}}\right)\frac{\partial^2\varphi_{i'}}{\partial x_j\partial x_r}(x,s),
\end{aligned} \tag{B.6}$$

for $s\geq 0$ and $1\leq i,j,r\leq d$.

(1) The first equation of (B.6) implies

$$\frac{\mathrm{d}}{\mathrm{d}s}\left(v_{lj}\frac{\partial\varphi_i}{\partial x_j}(x,s)\right) = -\left(a_{ir'}\frac{\partial^2 F}{\partial x_{r'}\partial x_{i'}}\right)\left(v_{lj}\frac{\partial\varphi_{i'}}{\partial x_j}(x,s)\right), \quad 1\leq l\leq d. \tag{B.7}$$

Since $\varphi(\cdot,0)$ is the identity map, we have

$$v_{lj}\frac{\partial\varphi_i}{\partial x_j}(x,0) = v_{li}, \quad \text{at } s=0. \tag{B.8}$$

Because $\boldsymbol{v}_l$ is the eigenvector of $a\nabla^2 F$, we can directly solve the solution of (B.7) and (B.8) and obtain

$$v_{lj}\frac{\partial\varphi_i}{\partial x_j}(x,s) = \mathrm{e}^{-\lambda_l s}v_{li} \iff \frac{\partial\varphi_i}{\partial x_j}(x,s) = \sum_{l=1}^{d}\mathrm{e}^{-\lambda_l s}v_{li}(a^{-1})_{jr}v_{lr}, \qquad \forall\ s\geq 0, \tag{B.9}$$

for $1 \le i, j \le d$. Sending $s \to +\infty$, using (B.2) and (B.3), we obtain

$$\frac{\partial \Theta_i}{\partial x_j} = \lim_{s\to+\infty} \frac{\partial \varphi_i}{\partial x_j}(x,s) = \sum_{l=1}^{d-k} v_{li}(a^{-1})_{jr} v_{lr} = P_{ij}. \tag{B.10}$$

(2) We proceed to compute $a_{jr}\frac{\partial^2 \Theta_i}{\partial x_j \partial x_r}$, $1 \le i \le d$. For this purpose, let us define

$$\begin{aligned} & A_l(x,s) = (a^{-1})_{ij'} v_{lj'} a_{jr} \frac{\partial^2 \varphi_i}{\partial x_j \partial x_r}(x,s), \quad 1 \le l \le d, \\ \iff & a_{jr}\frac{\partial^2 \varphi_i}{\partial x_j \partial x_r}(x,s) = \sum_{l=1}^{d} v_{li} A_l(x,s). \end{aligned}$$

Using the second equation of (B.6), the solution (B.9), and the orthogonality of the eigenvectors, we can obtain

$$\frac{\mathrm{d}A_l}{\mathrm{d}s}(x,s) = -\sum_{l'=1}^{d}\left[2\frac{\partial a_{ir}}{\partial x_{i'}}\frac{\partial^2 F}{\partial x_r \partial x_j}(a^{-1})_{ir'} + \frac{\partial^3 F}{\partial x_{r'}\partial x_{i'}\partial x_j}\right] v_{l'i'} v_{l'j} v_{lr'}\, \mathrm{e}^{-2\lambda_{l'}s} - \lambda_l A_l(x,s),$$

for $1 \le l \le d$, from which we get

$$\begin{aligned} & P_{ii'} a_{jr}\frac{\partial^2 \varphi_{i'}}{\partial x_j \partial x_r}(x,s) \\ & = \sum_{l=1}^{d-k} v_{li} A_l(x,s) \\ & = -\sum_{l=1}^{d-k}\sum_{l'=1}^{d}\left[2\frac{\partial a_{jr}}{\partial x_{i'}}\frac{\partial^2 F}{\partial x_r \partial x_{j'}}(a^{-1})_{jr'} + \frac{\partial^3 F}{\partial x_{r'}\partial x_{i'}\partial x_{j'}}\right] v_{l'i'} v_{l'j'} v_{lr'} v_{li}\, \mathrm{e}^{-\lambda_l s}\int_0^s \mathrm{e}^{(\lambda_l - 2\lambda_{l'})u}\,\mathrm{d}u \\ & = \sum_{l=1}^{d-k}\sum_{l'=1}^{d}\left[2\lambda_{l'}\frac{\partial (a^{-1})_{i'r}}{\partial x_j} - \frac{\partial^3 F}{\partial x_r \partial x_{i'}\partial x_j}\right] v_{l'i'} v_{l'j} v_{lr} v_{li}\int_0^s \mathrm{e}^{-2\lambda_{l'}u}\,\mathrm{d}u. \end{aligned}$$

To further simplify the last expression above, we differentiate the identity

$$\frac{\partial^2 F}{\partial x_{i'}\partial x_j} v_{l'i'} v_{l'j} = \lambda_{l'},$$

where l' is fixed, $1 \le l' \le d$, along the eigenvector $\boldsymbol{v}_l$, which gives

$$\begin{aligned} \frac{\partial^3 F}{\partial x_r \partial x_{i'}\partial x_j} v_{l'i'} v_{l'j} v_{lr} &= -2\frac{\partial^2 F}{\partial x_{i'}\partial x_j}\frac{\partial v_{l'i'}}{\partial x_r} v_{l'j} v_{lr} + \frac{\partial \lambda_{l'}}{\partial x_r} v_{lr} \\ &= -2\lambda_{l'}(a^{-1})_{i'r'} v_{l'r'}\frac{\partial v_{l'i'}}{\partial x_r} v_{lr} + \frac{\partial \lambda_{l'}}{\partial x_r} v_{lr}. \end{aligned}$$

Therefore, taking the limit $s \to +\infty$, using the relations (B.4), (B.5), and Lemma A.4, we can compute

$$\begin{aligned}
&P_{ii'}a_{jr}\frac{\partial^2\Theta_{i'}}{\partial x_j\partial x_r}\\
&= \lim_{s\to+\infty} P_{ii'}a_{jr}\frac{\partial^2\varphi_{i'}}{\partial x_j\partial x_r}(x,s)\\
&= \lim_{s\to+\infty}\sum_{l'=d-k+1}^{d}\sum_{l=1}^{d-k}\left[2\lambda_{l'}\frac{\partial(a^{-1})_{i'r}}{\partial x_j}v_{l'i'}v_{l'j}+2\lambda_{l'}(a^{-1})_{jr'}v_{l'r'}\frac{\partial v_{l'j}}{\partial x_r}-\frac{\partial\lambda_{l'}}{\partial x_r}\right]v_{lr}v_{li}\int_0^s \mathrm{e}^{-2\lambda_{l'}u}\,\mathrm{d}u\\
&= \frac{\partial(a^{-1})_{i'r}}{\partial x_j}\big(a_{i'j}-(Pa)_{i'j}\big)(Pa)_{ir}-\frac{1}{2}\frac{\partial(a^{-1})_{jr'}}{\partial x_r}\big(a_{jr'}-(Pa)_{jr'}\big)(Pa)_{ir}-\frac{1}{2}(Pa)_{ir}\frac{\partial\ln\det\Psi}{\partial x_r}\\
&= -P_{ir}\frac{\partial a_{jr}}{\partial x_j}-\frac{\partial P_{jr}}{\partial x_j}(Pa)_{ir}+P_{ir}\frac{\partial(Pa)_{jr}}{\partial x_j}+\frac{\partial P_{jr}}{\partial x_j}(Pa)_{ir}\\
&= -P_{ir}\frac{\partial a_{jr}}{\partial x_j}+P_{ir}\frac{\partial(Pa)_{jr}}{\partial x_j}.
\end{aligned}\tag{B.11}$$

On the other hand, differentiating the relation $\xi(\Theta(x))\equiv\mathbf{0}$ twice and using (B.10), we get

$$\frac{\partial\xi_\gamma}{\partial x_{i'}}\frac{\partial^2\Theta_{i'}}{\partial x_j\partial x_r}=-\frac{\partial^2\xi_\gamma}{\partial x_{i'}\partial x_{j'}}\frac{\partial\Theta_{i'}}{\partial x_j}\frac{\partial\Theta_{j'}}{\partial x_r}=-\frac{\partial^2\xi_\gamma}{\partial x_{i'}\partial x_{j'}}P_{i'j}P_{j'r},$$

for $1\le\gamma\le k$. Therefore, using $PaP^T=P^2a=Pa$ and $Pa\nabla\xi_\gamma=0$, we can compute

$$\begin{aligned}
(\delta_{ii'}-P_{ii'})a_{jr}\frac{\partial^2\Theta_{i'}}{\partial x_j\partial x_r}&=(\Psi^{-1})_{\alpha\gamma}(a\nabla\xi_\alpha)_i\frac{\partial\xi_\gamma}{\partial x_{i'}}a_{jr}\frac{\partial^2\Theta_{i'}}{\partial x_j\partial x_r}\\
&=-(\Psi^{-1})_{\alpha\gamma}(a\nabla\xi_\alpha)_i\frac{\partial^2\xi_\gamma}{\partial x_{i'}\partial x_{j'}}P_{i'j}P_{j'r}a_{jr}\\
&=-(\Psi^{-1})_{\alpha\gamma}(a\nabla\xi_\alpha)_i(\partial^2_{i'j'}\xi_\gamma)(Pa)_{i'j'}\\
&=(Pa)_{i'j'}\frac{\partial P_{ii'}}{\partial x_{j'}}.
\end{aligned}\tag{B.12}$$

Summing up (B.11) and (B.12), we conclude that

$$a_{jr}\frac{\partial^2\Theta_i}{\partial x_j\partial x_r}=\frac{\partial(Pa)_{ij}}{\partial x_j}-P_{ir}\frac{\partial a_{rj}}{\partial x_j}.$$

□

Now, we prove Theorem 3.5.

Proof of Theorem 3.5. Since we follow the approach in [35], we will only sketch the proof and will mainly focus on the differences.

First of all, we introduce some notations. Let $x^{(l)}$, $l=0,1,\ldots$, be the states generated from the numerical scheme (3.8) and let ψ be a function on Σ. We will adopt the abbreviations $\psi^{(l)}=\psi(x^{(l)})$, $P^{(l)}=P(x^{(l)})$, etc. For $j\ge1$, $D^j\psi[\boldsymbol{u}_1,\boldsymbol{u}_2,\ldots,\boldsymbol{u}_j]$ denotes the jth order directional derivatives of ψ along the vectors $\boldsymbol{u}_1$, $\boldsymbol{u}_2$, …, $\boldsymbol{u}_j$, and $|D^j\psi|_\infty$ is the supremum norm of $D^j\psi$ on Σ. Similarly, $D^j\Theta[\boldsymbol{u}_1,\boldsymbol{u}_2,\ldots,\boldsymbol{u}_j]$ denotes the d-dimensional vector whose ith component is $D^j\Theta_i[\boldsymbol{u}_1,\boldsymbol{u}_2,\ldots,\boldsymbol{u}_j]$, for $1\le i\le d$.

Define the vector $\boldsymbol{b}^{(l)}=(b_1^{(l)},b_2^{(l)},\ldots,b_d^{(l)})^T$ by

$$b_i^{(l)}=\left(-a_{ij}\frac{\partial U}{\partial x_j}+\frac{1}{\beta}\frac{\partial a_{ij}}{\partial x_j}\right)(x^{(l)}),\quad 1\le i\le d,\tag{B.13}$$

for $l = 0, 1, \ldots$, and set

$$\boldsymbol{\delta}^{(l)} = \boldsymbol{b}^{(l)} h + \sqrt{2\beta^{-1}h}\,\sigma^{(l)}\boldsymbol{\eta}^{(l)}. \tag{B.14}$$

We have

$$\boldsymbol{\delta}^{(l)} = x^{(l+\frac{1}{2})} - x^{(l)}, \qquad \text{and} \quad x^{(l+1)} = \Theta\big(x^{(l+\frac{1}{2})}\big) = \Theta\big(x^{(l)} + \boldsymbol{\delta}^{(l)}\big). \tag{B.15}$$

Let $\mathcal{L}$ be the infinitesimal generator of the SDE (2.5) in Theorem 2.3, given by

$$\begin{aligned} \mathcal{L} &= -(Pa)_{ij}\frac{\partial U}{\partial x_j}\frac{\partial}{\partial x_i} + \frac{1}{\beta}\frac{\partial (Pa)_{ij}}{\partial x_j}\frac{\partial}{\partial x_i} + \frac{1}{\beta}(Pa)_{ij}\frac{\partial^2}{\partial x_i \partial x_j} \\ &= \frac{\mathrm{e}^{\beta U}}{\beta}\frac{\partial}{\partial x_i}\left(\mathrm{e}^{-\beta U}(Pa)_{ij}\frac{\partial}{\partial x_j}\right), \end{aligned} \tag{B.16}$$

in Remark 2.5. We consider the Poisson equation on Σ

$$\mathcal{L}\psi = f - \overline{f}. \tag{B.17}$$

The existence and the regularity of the solution ψ can be established under Assumption 1.1 and 1.2, and the Bakry-Emery condition in Section 2. Applying Taylor's theorem and using the fact that $\Theta(x^{(l)}) = x^{(l)}$ since $x^{(l)} \in \Sigma$, we have

$$\begin{aligned} \psi^{(l+1)} &= (\psi \circ \Theta)\big(x^{(l)} + \boldsymbol{\delta}^{(l)}\big) \\ &= \psi^{(l)} + D(\psi \circ \Theta)^{(l)}[\boldsymbol{\delta}^{(l)}] + \frac{1}{2}D^2(\psi \circ \Theta)^{(l)}[\boldsymbol{\delta}^{(l)}, \boldsymbol{\delta}^{(l)}] + \frac{1}{6}D^3(\psi \circ \Theta)^{(l)}[\boldsymbol{\delta}^{(l)}, \boldsymbol{\delta}^{(l)}, \boldsymbol{\delta}^{(l)}] + R^{(l)}, \end{aligned} \tag{B.18}$$

where the reminder is given by

$$R^{(l)} = \frac{1}{6}\left(\int_0^1 s^3\, D^4(\psi \circ \Theta)\big(x^{(l)} + (1-s)\boldsymbol{\delta}^{(l)}\big)\,\mathrm{d}s\right)\left[\boldsymbol{\delta}^{(l)}, \boldsymbol{\delta}^{(l)}, \boldsymbol{\delta}^{(l)}, \boldsymbol{\delta}^{(l)}\right].$$

Now we apply Proposition 3.4 to simplify the expression in (B.18). Using the chain rule, the expressions (B.14)–(B.16), we can derive

$$\begin{aligned} &\psi^{(l+1)} \\ &= \psi^{(l)} + D\psi^{(l)}\left[P^{(l)}\boldsymbol{\delta}^{(l)} + \frac{1}{2}D^2\Theta^{(l)}[\boldsymbol{\delta}^{(l)}, \boldsymbol{\delta}^{(l)}]\right] + \frac{1}{2}D^2\psi^{(l)}[P^{(l)}\boldsymbol{\delta}^{(l)}, P^{(l)}\boldsymbol{\delta}^{(l)}] \\ &\quad + \frac{1}{6}D^3(\psi \circ \Theta)^{(l)}[\boldsymbol{\delta}^{(l)}, \boldsymbol{\delta}^{(l)}, \boldsymbol{\delta}^{(l)}] + R^{(l)} \\ &= \psi^{(l)} + (\mathcal{L}\psi)^{(l)}h + \sqrt{2\beta^{-1}h}\,D\psi^{(l)}[(P\sigma)^{(l)}\boldsymbol{\eta}^{(l)}] + \frac{h^2}{2}D\psi^{(l)}\left[D^2\Theta^{(l)}[\boldsymbol{b}^{(l)}, \boldsymbol{b}^{(l)}]\right] \\ &\quad + \sqrt{2\beta^{-1}}h^{\frac{3}{2}}D\psi^{(l)}\left[D^2\Theta^{(l)}[\boldsymbol{b}^{(l)}, \sigma^{(l)}\boldsymbol{\eta}^{(l)}]\right] + \frac{h^2}{2}D^2\psi^{(l)}[P^{(l)}\boldsymbol{b}^{(l)}, P^{(l)}\boldsymbol{b}^{(l)}] \\ &\quad + \sqrt{2\beta^{-1}}h^{\frac{3}{2}}D^2\psi^{(l)}[P^{(l)}\boldsymbol{b}^{(l)}, (P\sigma)^{(l)}\boldsymbol{\eta}^{(l)}] + \frac{hD\psi^{(l)}}{\beta}\left[D^2\Theta^{(l)}[\sigma^{(l)}\boldsymbol{\eta}^{(l)}, \sigma^{(l)}\boldsymbol{\eta}^{(l)}] - a^{(l)} : \nabla^2\Theta^{(l)}\right] \\ &\quad + \frac{h}{\beta}\left(D^2\psi^{(l)}[(P\sigma)^{(l)}\boldsymbol{\eta}^{(l)}, (P\sigma)^{(l)}\boldsymbol{\eta}^{(l)}] - (Pa)^{(l)} : D^2\psi^{(l)}\right) + \frac{1}{6}D^3(\psi \circ \Theta)^{(l)}[\boldsymbol{\delta}^{(l)}, \boldsymbol{\delta}^{(l)}, \boldsymbol{\delta}^{(l)}] + R^{(l)}, \end{aligned} \tag{B.19}$$

where in the last equation we added and subtracted some terms, and we used the identity

$$D\psi^{(l)}\left[P^{(l)}\boldsymbol{b}^{(l)} + \frac{1}{\beta}a^{(l)} : \nabla^2\Theta^{(l)}\right] + \frac{1}{\beta}(Pa)^{(l)} : \nabla^2\psi^{(l)} = (\mathcal{L}\psi)^{(l)}, \tag{B.20}$$

which can be verified using Proposition 3.4, (B.13) and (B.16). In (B.20), $a : \nabla^2\Theta$ is the vector whose ith component is given by $a_{jr}\frac{\partial^2\Theta_i}{\partial x_j \partial x_r}$, and $(Pa) : \nabla^2\psi$ is defined in a similar way.

Summing up (B.19) for $l = 0, 1, \ldots, n-1$, dividing both sides by T, and using the Poisson equation (B.17), gives

$$\widehat{f}_n - \overline{f} = \frac{1}{n}\sum_{l=0}^{n-1} f(x^{(l)}) - \overline{f} = \frac{\psi^{(n)} - \psi^{(0)}}{T} + \frac{1}{T}\sum_{i=1}^{5} M_{i,n} + \frac{1}{T}\sum_{i=1}^{4} S_{i,n}, \tag{B.21}$$

where

$$\begin{aligned}
M_{1,n} &= -\sqrt{2\beta^{-1}h}\sum_{l=0}^{n-1} D\psi^{(l)}[(P\sigma)^{(l)}\boldsymbol{\eta}^{(l)}],\\
M_{2,n} &= -\sqrt{2\beta^{-1}}h^{\frac{3}{2}}\sum_{l=0}^{n-1} D\psi^{(l)}\left[D^2\Theta^{(l)}[\boldsymbol{b}^{(l)}, \sigma^{(l)}\boldsymbol{\eta}^{(l)}]\right],\\
M_{3,n} &= -\frac{h}{\beta}\sum_{l=0}^{n-1} D\psi^{(l)}\left[D^2\Theta^{(l)}[\sigma^{(l)}\boldsymbol{\eta}^{(l)}, \sigma^{(l)}\boldsymbol{\eta}^{(l)}] - a^{(l)} : \nabla^2\Theta^{(l)}\right],\\
M_{4,n} &= -\sqrt{2\beta^{-1}}h^{\frac{3}{2}}\sum_{l=0}^{n-1} D^2\psi^{(l)}\left[P^{(l)}\boldsymbol{b}^{(l)}, (P\sigma)^{(l)}\boldsymbol{\eta}^{(l)}\right],\\
M_{5,n} &= -\frac{h}{\beta}\sum_{l=0}^{n-1}\left(D^2\psi^{(l)}\left[(P\sigma)^{(l)}\boldsymbol{\eta}^{(l)}, (P\sigma)^{(l)}\boldsymbol{\eta}^{(l)}\right] - (Pa)^{(l)} : D^2\psi^{(l)}\right),
\end{aligned} \tag{B.22}$$

and

$$\begin{aligned}
S_{1,n} &= -\frac{h^2}{2}\sum_{l=0}^{n-1} D\psi^{(l)}\left[D^2\Theta^{(l)}[\boldsymbol{b}^{(l)}, \boldsymbol{b}^{(l)}]\right],\\
S_{2,n} &= -\frac{h^2}{2}\sum_{l=0}^{n-1} D^2\psi^{(l)}\left[P^{(l)}\boldsymbol{b}^{(l)}, P^{(l)}\boldsymbol{b}^{(l)}\right],\\
S_{3,n} &= -\sum_{l=0}^{n-1} R^{(l)}, \qquad S_{4,n} = -\frac{1}{6}\sum_{l=0}^{n-1} D^3(\psi\circ\Theta)^{(l)}\left[\boldsymbol{\delta}^{(l)}, \boldsymbol{\delta}^{(l)}, \boldsymbol{\delta}^{(l)}\right].
\end{aligned} \tag{B.23}$$

Using (B.14), the last term $S_{4,n}$ above can be further decomposed as

$$S_{4,n} = M_{0,n} + S_{0,n},$$

where

$$\begin{aligned}
M_{0,n} &= -\frac{\sqrt{2\beta^{-1}}}{6}h^{\frac{3}{2}}\sum_{l=0}^{n-1}\left(\frac{2}{\beta}D^3(\psi\circ\Theta)^{(l)}\left[\sigma^{(l)}\boldsymbol{\eta}^{(l)}, \sigma^{(l)}\boldsymbol{\eta}^{(l)}, \sigma^{(l)}\boldsymbol{\eta}^{(l)}\right] + 3hD^3(\psi\circ\Theta)^{(l)}\left[\boldsymbol{b}^{(l)}, \boldsymbol{b}^{(l)}, \sigma^{(l)}\boldsymbol{\eta}^{(l)}\right]\right),\\
S_{0,n} &= -\frac{h^2}{6}\sum_{l=0}^{n-1}\left(\frac{6}{\beta}D^3(\psi\circ\Theta)^{(l)}\left[\boldsymbol{b}^{(l)}, \sigma^{(l)}\boldsymbol{\eta}^{(l)}, \sigma^{(l)}\boldsymbol{\eta}^{(l)}\right] + hD^3(\psi\circ\Theta)^{(l)}\left[\boldsymbol{b}^{(l)}, \boldsymbol{b}^{(l)}, \boldsymbol{b}^{(l)}\right]\right).
\end{aligned} \tag{B.24}$$

Notice that the terms $M_{i,n}$, $0 \le i \le 5$, are all martingales and in particular we have $\mathbf{E}M_{i,n} = 0$. Therefore, since the level set Σ is compact (Assumption 1.2), the first conclusion follows from the estimates

$$\begin{aligned}
&|S_{1,n}| \le C|D\psi|_\infty\, h\, T, && |S_{2,n}| \le C|D^2\psi|_\infty\, h\, T,\\
&\mathbf{E}|S_{0,n}| \le C|D^3\psi|_\infty\, h\, T, && \mathbf{E}|S_{3,n}| \le C|D^4\psi|_\infty\, h\, T,
\end{aligned} \tag{B.25}$$

while the second conclusion follows by squaring both sides of (B.21) and using the estimates

$$\begin{aligned}
&\mathbf{E}|S_{0,n}|^2 \le Ch^2T^2|D^3\psi|_\infty^2, && \mathbf{E}|S_{3,n}|^2 \le Ch^2T^2|D^4\psi|_\infty^2, && \\
&\mathbf{E}|M_{0,n}|^2 \le Ch^2T|D^3\psi|_\infty^2, && \mathbf{E}|M_{1,n}|^2 \le CT|D\psi|_\infty^2, && \mathbf{E}|M_{2,n}|^2 \le Ch^2T|D\psi|_\infty^2, \\
&\mathbf{E}|M_{3,n}|^2 \le ChT|D\psi|_\infty^2, && \mathbf{E}|M_{4,n}|^2 \le Ch^2T|D^2\psi|_\infty^2, && \mathbf{E}|M_{5,n}|^2 \le ChT|D^2\psi|_\infty^2.
\end{aligned} \tag{B.26}$$

As far as the third conclusion (pathwise estimate) is concerned, notice that (B.21) implies

$$\begin{aligned}
|\widehat{f}_n - \overline{f}| &\le \frac{|\psi^{(n)} - \psi^{(0)}|}{T} + \frac{1}{T}\sum_{i=0}^{5}|M_{i,n}| + \frac{1}{T}\sum_{i=0}^{3}|S_{i,n}| \\
&\le C\left(h + \frac{1}{T}\right) + \frac{1}{T}\sum_{i=0}^{5}|M_{i,n}|,
\end{aligned} \tag{B.27}$$

where we have used the estimates (B.25) for $|S_{1,n}|$, $|S_{2,n}|$, and the upper bounds

$$\begin{aligned}
|S_{0,n}| &\le Ch^2\sum_{l=0}^{n-1}|\boldsymbol{\eta}^{(l)}|^2 + Ch^3n \le ChT, \quad a.s. \\
|S_{3,n}| &\le Ch^2\sum_{l=0}^{n-1}|\boldsymbol{\eta}^{(l)}|^4 + Ch^4n \le ChT, \quad a.s.
\end{aligned}$$

which are implied by the strong law of large numbers for $\frac{1}{n}\sum_{l=0}^{n-1}|\boldsymbol{\eta}^{(l)}|^4$, when $n \to +\infty$. Finally, we estimate the martingale terms $M_{i,n}$ in (B.27). Notice that, for any $r \ge 1$, we can deduce the following upper bounds (see [35])

$$\begin{aligned}
&\frac{1}{T^{2r}}\mathbf{E}|M_{1,n}|^{2r} \le \frac{C}{T^r}, \quad \frac{1}{T^{2r}}\mathbf{E}|M_{2,n}|^{2r} \le \frac{Ch^{2r}}{T^r}, \\
&\frac{1}{T^{2r}}\mathbf{E}|M_{3,n}|^{2r} \le \frac{Ch^r}{T^r}, \quad \frac{1}{T^{2r}}\mathbf{E}|M_{4,n}|^{2r} \le \frac{Ch^{2r}}{T^r}, \\
&\frac{1}{T^{2r}}\mathbf{E}|M_{5,n}|^{2r} \le \frac{Ch^r}{T^r}, \quad \frac{1}{T^{2r}}\mathbf{E}|M_{0,n}|^{2r} \le \frac{Ch^{2r}}{T^r},
\end{aligned}$$

which give

$$\mathbf{E}\left(\frac{1}{T}\sum_{i=0}^{5}|M_{i,n}|\right)^{2r} \le \frac{C}{T^{2r}}\sum_{i=0}^{5}\mathbf{E}|M_{i,n}|^{2r} \le \frac{C}{T^r}. \tag{B.28}$$

Now, for any $0 < \epsilon < \frac{1}{2}$, the Borel–Cantelli lemma implies that there is an almost surely bounded random variable $\zeta(\omega)$, such that

$$\frac{1}{T}\sum_{i=0}^{5}|M_{i,n}| \le \frac{\zeta(\omega)}{T^{\frac{1}{2}-\epsilon}}. \tag{B.29}$$

Therefore, the third conclusion follows readily from (B.27) and (B.29). □

Next, we prove Corollary 3.7.

Proof of Corollary 3.7. From the estimates in (B.26), we know that it is only necessary to consider the term $M_{1,n}$ in (B.22). Recall that ψ solves the Poisson equation (B.17) and we can assume $\int_\Sigma \psi \, \mathrm{d}\mu_1 = 0$ without loss

of generosity. Applying the Poisson equation, the Poincaré inequality, and the Cauchy-Schwarz inequality, we have the standard estimates

$$\begin{aligned}\int_\Sigma \psi^2 \,\mathrm{d}\mu_1 &\le -\frac{1}{K}\int_\Sigma (\mathcal{L}\psi)\psi \,\mathrm{d}\mu_1 \\ &\le \frac{1}{K}\left[\int_\Sigma (\mathcal{L}\psi)^2 \,\mathrm{d}\mu_1\right]^{\frac{1}{2}}\left(\int_\Sigma \psi^2 \,\mathrm{d}\mu_1\right)^{\frac{1}{2}} \\ &= \frac{1}{K}\left[\int_\Sigma (f-\overline{f})^2 \,\mathrm{d}\mu_1\right]^{\frac{1}{2}}\left(\int_\Sigma \psi^2 \,\mathrm{d}\mu_1\right)^{\frac{1}{2}},\end{aligned}$$

which implies

$$\left(\int_\Sigma \psi^2 \,\mathrm{d}\mu_1\right)^{\frac{1}{2}} \le \frac{1}{K}\left[\int_\Sigma (f-\overline{f})^2 \,\mathrm{d}\mu_1\right]^{\frac{1}{2}}, \quad \text{and} \quad -\int_\Sigma (\mathcal{L}\psi)\psi \,\mathrm{d}\mu_1 \le \frac{1}{K}\int_\Sigma (f-\overline{f})^2 \,\mathrm{d}\mu_1. \tag{B.30}$$

Since the term $M_{1,n}$ in (B.22) is a martingale, we have

$$\frac{1}{T^2}\mathbf{E}|M_{1,n}|^2 = \frac{2\beta^{-1}}{T}\frac{1}{n}\sum_{l=0}^{n-1}\mathbf{E}\left[\left((Pa)^{(l)}\nabla\psi^{(l)}\right)\cdot\nabla\psi^{(l)}\right].$$

Applying the first estimate in the conclusion of Theorem 3.5, using (2.9) in Remark 2.5, as well as the estimate (B.30), we obtain

$$\begin{aligned}\frac{1}{T^2}\mathbf{E}|M_{1,n}|^2 &\le \frac{2\beta^{-1}}{T}\int_\Sigma (Pa\nabla\psi)\cdot\nabla\psi \,\mathrm{d}\mu_1 + C\left(\frac{h}{T}+\frac{1}{T^2}\right) \\ &\le \frac{2\int_\Sigma (f-\overline{f})^2 \,\mathrm{d}\mu_1}{KT} + C\left(\frac{h}{T}+\frac{1}{T^2}\right).\end{aligned}$$

The conclusion follows by squaring both sides of (B.21), applying Young's inequality, and using the same argument of Theorem 3.5. □

Finally, we prove Proposition 3.10, which concerns the properties of the projection map Π defined in (3.19).

Proof of Proposition 3.10. For $1 \le l \le d$, recall that $\boldsymbol{p}_l = (P\sigma)_{i'l}\boldsymbol{e}_{i'}$ is the tangent vector field defined in Appendix A such that $\boldsymbol{p}_l \in T_x\Sigma$ at each $x \in \Sigma$. Since $\Pi_i(x) = x_i$ for $x \in \Sigma$, $1 \le i \le d$, taking derivatives along $\boldsymbol{p}_l$ twice, we obtain

$$\begin{aligned}\frac{\partial \Pi_i}{\partial x_j}(P\sigma)_{jl} &= (P\sigma)_{il}, \\ \frac{\partial^2 \Pi_i}{\partial x_j \partial x_r}(P\sigma)_{jl}(P\sigma)_{rl} &= (P\sigma)_{rl}\frac{\partial (P\sigma)_{il}}{\partial x_r} - \frac{\partial \Pi_i}{\partial x_j}(P\sigma)_{rl}\frac{\partial (P\sigma)_{jl}}{\partial x_r}.\end{aligned} \tag{B.31}$$

Notice that, for a function which only depends on the state and is evaluated at $x \in \Sigma$, we will often omit its argument in order to keep the notations simple.

On the other hand, the vector $\boldsymbol{\sigma}_l - \boldsymbol{p}_l = ((I-P)\sigma)_{i'l}\boldsymbol{e}_{i'} \in (T_x\Sigma)^\perp$ (the complement of the subspace $T_x\Sigma$ in $T_x\mathcal{M}$). Let $\phi(s)$ be the geodesic curve in $\mathcal{M}$ such that $\phi(0) = x$ and $\phi'(0) = \boldsymbol{\sigma}_l - \boldsymbol{p}_l$. We have $\Pi_i(\phi(s)) = x_i$, $\forall s \in [0,\epsilon)$ for some $\epsilon > 0$. Taking derivatives with respect to s twice, we obtain

$$\begin{aligned}&\frac{\partial \Pi_i}{\partial x_j}(\phi(s))\frac{\mathrm{d}\phi_j(s)}{\mathrm{d}s} = 0, \\ &\frac{\partial^2 \Pi_i}{\partial x_j \partial x_r}(\phi(s))\frac{\mathrm{d}\phi_j(s)}{\mathrm{d}s}\frac{\mathrm{d}\phi_r(s)}{\mathrm{d}s} = -\frac{\partial \Pi_i}{\partial x_j}(\phi(s))\frac{\mathrm{d}^2\phi_j(s)}{\mathrm{d}s^2} = \frac{\partial \Pi_i}{\partial x_j}(\phi(s))\,\Gamma^j_{rr'}(\phi(s))\frac{\mathrm{d}\phi_r(s)}{\mathrm{d}s}\frac{\mathrm{d}\phi_{r'}(s)}{\mathrm{d}s},\end{aligned}$$

for $1 \le i \le d$, where ϕ_j denotes the jth component of ϕ, and the geodesic equation of the curve ϕ has been used to obtain the last expression above. In particular, setting $s = 0$, we obtain

$$\begin{aligned} \frac{\partial \Pi_i}{\partial x_j}\big(\sigma_{jl} - (P\sigma)_{jl}\big) &= 0, \\ \frac{\partial^2 \Pi_i}{\partial x_j \partial x_r}\big(\sigma_{jl} - (P\sigma)_{jl}\big)\big(\sigma_{rl} - (P\sigma)_{rl}\big) &= \frac{\partial \Pi_i}{\partial x_j}\Gamma^j_{rr'}\big(\sigma_{rl} - (P\sigma)_{rl}\big)\big(\sigma_{r'l} - (P\sigma)_{r'l}\big). \end{aligned} \tag{B.32}$$

Combining the first equations in both (B.31) and (B.32), we can conclude that $\frac{\partial \Pi_i}{\partial x_j} = P_{ij}$ at $x \in \Sigma$. Since (B.32) holds at any $x \in \Sigma$, taking the derivative in the first equation of (B.32) along the tangent vector $\boldsymbol{p}_l \in T_x\Sigma$, we obtain

$$\frac{\partial^2 \Pi_i}{\partial x_j \partial x_r}\big(\sigma_{jl} - (P\sigma)_{jl}\big)(P\sigma)_{rl} = -\frac{\partial \Pi_i}{\partial x_j}(P\sigma)_{rl}\frac{\partial\big(\sigma_{jl} - (P\sigma)_{jl}\big)}{\partial x_r}. \tag{B.33}$$

Combining (B.31)–(B.33), using Lemma A.4, the expression in (A.5), the relations

$$\begin{aligned} (P\sigma)_{jl}(P\sigma)_{rl} &= (PaP^T)_{jr} = (Pa)_{jr}, \\ \big(\sigma_{rl} - (P\sigma)_{rl}\big)\big(\sigma_{r'l} - (P\sigma)_{r'l}\big) &= a_{rr'} - (Pa)_{rr'}, \end{aligned}$$

and the integration by parts formula, we can compute

$$\begin{aligned} &\frac{\partial^2 \Pi_i}{\partial x_j \partial x_r} a_{jr} \\ &\frac{\partial^2 \Pi_i}{\partial x_j \partial x_r}\big(P\sigma + (\sigma - P\sigma)\big)_{jl}\big(P\sigma + (\sigma - P\sigma)\big)_{rl} \\ &\quad = \frac{\partial^2 \Pi_i}{\partial x_j \partial x_r}(P\sigma)_{jl}(P\sigma)_{rl} + 2\frac{\partial^2 \Pi_i}{\partial x_j \partial x_r}(\sigma - P\sigma)_{jl}(P\sigma)_{rl} + \frac{\partial^2 \Pi_i}{\partial x_j \partial x_r}(\sigma - P\sigma)_{jl}(\sigma - P\sigma)_{rl} \\ &\quad = (P\sigma)_{rl}\frac{\partial (P\sigma)_{il}}{\partial x_r} - P_{ij}(P\sigma)_{rl}\frac{\partial (P\sigma)_{jl}}{\partial x_r} - 2P_{ij}(P\sigma)_{rl}\frac{\partial\big(\sigma_{jl} - (P\sigma)_{jl}\big)}{\partial x_r} \\ &\qquad + P_{ij}\Gamma^j_{rr'}\big(\sigma_{rl} - (P\sigma)_{rl}\big)\big(\sigma_{r'l} - (P\sigma)_{r'l}\big) \\ &\quad = \left[(P\sigma)_{rl}\frac{\partial (P\sigma)_{il}}{\partial x_r} + P_{ij}(P\sigma)_{rl}\frac{\partial (P\sigma)_{jl}}{\partial x_r} - 2P_{ij}(P\sigma)_{rl}\frac{\partial \sigma_{jl}}{\partial x_r}\right] + P_{ij}\Gamma^j_{rr'}\big(a_{rr'} - (Pa)_{rr'}\big) \\ &\quad = \left[2(P\sigma)_{rl}\frac{\partial (P\sigma)_{il}}{\partial x_r} - (P\sigma)_{jl}(P\sigma)_{rl}\frac{\partial P_{ij}}{\partial x_r} - 2(P\sigma)_{rl}\frac{\partial (P\sigma)_{il}}{\partial x_r} + 2(P\sigma)_{rl}\sigma_{jl}\frac{\partial P_{ij}}{\partial x_r}\right] \\ &\qquad + (Pa)_{ij}\frac{\partial (a^{-1})_{lj}}{\partial x_r}\big(a_{lr} - (Pa)_{lr}\big) - \frac{1}{2}(Pa)_{ij}\frac{\partial (a^{-1})_{lr}}{\partial x_j}\big(a_{lr} - (Pa)_{lr}\big) \\ &\quad = (Pa)_{lj}\frac{\partial P_{ij}}{\partial x_l} + \left[-P_{ij}\frac{\partial a_{jl}}{\partial x_l} - (Pa)_{ij}\frac{\partial P_{lj}}{\partial x_l} + P_{il}\frac{\partial (Pa)_{lj}}{\partial x_j}\right] + (Pa)_{ij}\frac{\partial P_{lj}}{\partial x_l} + \frac{1}{2}(Pa)_{ij}\frac{\partial \ln\det\Psi}{\partial x_j} \\ &\quad = -P_{ij}\frac{\partial a_{jl}}{\partial x_l} + \frac{\partial (Pa)_{ij}}{\partial x_j} + \frac{1}{2}(Pa)_{ij}\frac{\partial \ln\det\Psi}{\partial x_j}. \end{aligned}$$

□

Acknowledgements. This work is funded by the Einstein Center of Mathematics (ECMath) through project CH21. The author would like to thank Gabriel Stoltz for stimulating discussions on constrained Langevin processes at the Institut Henri Poincaré – Centre Émile Borel during the trimester "Stochastic Dynamics Out of Equilibrium". The author appreciates the hospitality of this institution. The author also thanks the anonymous referees for their valuable comments and criticism which helped improve the manuscript substantially.

References

[1] A. Abdulle, G. Vilmart and K. Zygalakis, High order numerical approximation of the invariant measure of ergodic SDEs. *SIAM J. Numer. Anal.* **52** (2014) 1600–1622.

[2] L. Ambrosio and H.M. Soner, Level set approach to mean curvature flow in arbitrary codimension. *J. Differ. Geom.* **43** (1996) 693–737.

[3] L. Ambrosio, N. Gigli and G. Savaré. Gradient flows: in metric spaces and in the space of probability measures. In: *Lectures in Mathematics*. Birkhäuser (2005).

[4] D. Bakry and M. Émery, Hypercontractivité de semi-groupes de diffusion. *C. R. Math. Acad. Sci. Paris, Ser. I* **299** (1984) 775–778.

[5] A. Banyaga and D. Hurtubise, In: *Lectures on Morse Homology. Texts in the Mathematical Sciences*. Springer Netherlands (2004).

[6] R.L. Bishop and R.J. Crittenden, Geometry of Manifolds. In: *AMS/Chelsea Publication Series*. American Mathematical Society (1964).

[7] N. Bou-Rabee and H. Owhadi, Long-run accuracy of variational integrators in the stochastic context. *SIAM J. Numer. Anal.* **48** (2010) 278–297.

[8] M. Brubaker, M. Salzmann and R. Urtasun, A family of MCMC methods on implicitly defined manifoldsm, edited by N.D. Lawrence and M. Girolami. In: Proceedings of the Fifteenth International Conference on Artificial Intelligence and Statistics. Vol. 22 of *Proceedings of Machine Learning Research*. PMLR (2012) 161–172.

[9] G. Ciccotti, R. Kapral and E. Vanden-Eijnden, Blue moon sampling, vectorial reaction coordinates, and unbiased constrained dynamics. *ChemPhysChem* **6** (2005) 1809–1814.

[10] G. Ciccotti, T. Lelièvre and E. Vanden-Eijnden, Projection of diffusions on submanifolds: application to mean force computation. *Commun. Pur. Appl. Math.* **61** (2008) 371–408.

[11] A. Debussche and E. Faou, Weak backward error analysis for SDEs. *SIAM J. Numer. Anal.* **50** (2012) 1735–1752.

[12] M.P. do Carmo, Riemannian Geometry. Mathematics. Birkhäuser, Boston, MA (1992).

[13] I. Fatkullin, G. Kovacic and E. Vanden-Eijnden, Reduced dynamics of stochastically perturbed gradient flows. *Commun. Math. Sci.* **8** (2010) 439–461.

[14] G. Froyland, G.A. Gottwald and A. Hammerlindl. A computational method to extract macroscopic variables and their dynamics in multiscale systems. *SIAM J. Appl. Dyn. Syst.* **13** (2014) 1816–1846.

[15] T. Funaki and H. Nagai, Degenerative convergence of diffusion process toward a submanifold by strong drift. *Stoch. Stoch. Rep.* **44** (1993) 1–25.

[16] M. Girolami and B. Calderhead. Riemann manifold Langevin and Hamiltonian Monte Carlo methods. *J. R. Stat. Soc. B.* **73** (2011) 123–214.

[17] D. Givon, R. Kupferman and A.M. Stuart, Extracting macroscopic dynamics: model problems and algorithms. *Nonlinearity* **17** (2004) R55–R127.

[18] I. Gyöngy, Mimicking the one-dimensional marginal distributions of processes having an Ito differential. *Probab. Th. Rel. Fields* **71** (1986) 501–516.

[19] C. Hartmann, C. Schütte and W. Zhang, Jarzynski equality, fluctuation theorem, and variance reduction: mathematical analysis and numerical algorithms. *J. Stat. Phys.* **175** (2019) 1214–1261.

[20] E.P. Hsu, Stochastic analysis on manifolds. In: *Graduate Studies in Mathematics*. American Mathematical Society (2002).

[21] J. Jost, Riemannian Geometry and Geometric Analysis. Universitext. Springer Berlin Heidelberg (2008).

[22] G.S. Katzenberger, Solutions of a stochastic differential equation forced onto a manifold by a large drift. *Ann. Probab.* **19** (1991) 1587–1628.

[23] I.G. Kevrekidis and G. Samaey, Equation-free multiscale computation: algorithms and applications. *Annu. Rev. Phys. Chem.* **60** (2009) 321–344.

[24] I.G. Kevrekidis, C.W. Gear, J.M. Hyman, P.G Kevrekidid, O. Runborg and C. Theodoropoulos, Equation-free, coarse-grained multiscale computation: enabling mocroscopic simulators to perform system-level analysis. *Commun. Math. Sci.* **1** (2003) 715–762.

[25] I.G. Kevrekidis, C.W. Gear and G. Hummer, Equation-free: the computer-aided analysis of complex multiscale systems. *AIChE J.* **50** (2004) 1346–1355.

[26] F. Legoll and T. Lelièvre, Effective dynamics using conditional expectations. *Nonlinearity* **23** (2010) 2131–2163.

[27] B. Leimkuhler and C. Matthews, Efficient molecular dynamics using geodesic integration and solvent–solute splitting. *Proc. Math. Phys. Eng. Sci.* **472** (2016) 20160138.

[28] B. Leimkuhler, C. Matthews and G. Stoltz, The computation of averages from equilibrium and nonequilibrium Langevin molecular dynamics. *IMA J. Numer. Anal.* **36** (2016) 13–79.

[29] T. Lelièvre and W. Zhang, Pathwise estimates for effective dynamics: the case of nonlinear vectorial reaction coordinates. Preprint arXiv:1805.01928 (2018).

[30] T. Lelièvre, M. Rousset and G. Stoltz, Free Energy Computations: A Mathematical Perspective. Imperial College Press (2010).

[31] T. Lelièvre, M. Rousset and G. Stoltz, Langevin dynamics with constraints and computation of free eneregy differences. *Math. Comput.* **81** (2012) 2071–2125.

[32] T. Lelievre, M. Rousset and G. Stoltz, Hybrid Monte Carlo methods for sampling probability measures on submanifolds. Preprint arXiv:1807.02356 (2018).

[33] A.J. Majda, C. Franzke and B. Khouider, An applied mathematics perspective on stochastic modelling for climate. *Philos. Trans. R. Soc. A* **366** (2008) 2429–2455.

[34] L. Maragliano and E. Vanden-Eijnden, A temperature accelerated method for sampling free energy and determining reaction pathways in rare events simulations. *Chem. Phys. Lett.* **426** (2006) 168–175.

[35] J.C. Mattingly, A.M. Stuart and M.V. Tretyakov, Convergence of numerical time-averaging and stationary measures via Poisson equations. *SIAM J. Numer. Anal.* **48** (2010) 552–577.

[36] G.A. Pavliotis and A.M. Stuart, In: Multiscale Methods: Averaging and Homogenization. *Texts in Applied Mathematics*. Springer New York (2008).

[37] P. Petersen, Riemannian Geometry. In: *Graduate Texts in Mathematics*. Springer New York (2006).

[38] K.B. Petersen and M.S. Pedersen, The Matrix Cookbook. http://www2.imm.dtu.dk/pubdb/p.php?3274 (2012). Version 20121115.

[39] K.T. Sturm, Convex functionals of probability measures and nonlinear diffusions on manifolds. *J. Math. Pures Appl.* **84** (2005) 149–168.

[40] D. Talay and L. Tubaro, Expansion of the global error for numerical schemes solving stochastic differential equations. *Stoch. Anal. Appl.* **8** (1990) 483–509.

[41] E. Vanden-Eijnden, Numerical techniques for multi-scale dynamical systems with stochastic effects. *Commun. Math. Sci.* **1** (2003) 385–391.

[42] E. Weinan, B. Engquist, X. Li, W. Ren and E. Vanden-Eijnden, Heterogeneous multiscale methods: a review. *Commun. Comput. Phys.* **2** (2007) 367–450.

[43] E. Zappa, M. Holmes-Cerfon and J. Goodman, Monte Carlo on manifolds: sampling densities and integrating functions. *Commun. Pure Appl. Math.* **71** (2018) 2609–2647.

[44] W. Zhang, C. Hartmann and C. Schütte, Effective dynamics along given reaction coordinates, and reaction rate theory. *Faraday Discuss.* **195** (2016) 365–394.